PART IV

RESULTS OF RADIOLYTIC GAS PRODUCTION

RADIOLYTICAL GAS PRODUCTION OF ROCK SALT AFTER IRRADIATION WITH Co-60 SOURCES: POTASAS DEL LLOBREGAT SAMPLES

C.de las Cuevas, P.Teixidor, L.Miralles

ABSTRACT

The production of gas resulting from exposure of rock salt to gamma irradiation has been studied. In order to discern which gases come from radiolysis and which are related to thermal desorption, two sets of experiments were conducted. The first set of experiments consisted of laboratory degasification tests at 50ºC, and the second consisted of irradiations using Co^{60} sources at the same temperature. CO_2, H_2, NO_x, SO_x, O_2, CH_4 and chlorine-bearing gases were determined. The obtained results, allowed us to identify gases arising from the radiolysis of organic matter and brine, and also those arising from radiolytical oxidation. In addition, certain amounts of the produced chlorine-bearing gases were trapped inside the halite crystals.

1. INTRODUCTION

After the disposal of radioactive waste in rock salt, the waste acts as a source of heat and radiation. The emplacement of waste gives rise to a temporary local heating (the first 10 years) and a long lasting general heating of the surrounding rock salt (about the first 1000 years). As a result of the high temperature, primary gases and gases generated by the thermal decomposition of the organic matter are released. In addition to the effect of temperature, gamma-radiation will be responsible for the generation of radiation induced defects in the NaCl crystal and the production of radiolytical gases arising basically from the decomposition of organic matter and brine.

When NaCl is irradiated, the ionization causes Cl^- ions to be ejected from their normal lattice sites to form interstitial chlorine atoms (H-centre) and empty lattice sites. The empty lattice site traps the electron left behind (F-centre), preserving the neutrality of the crystal. At temperatures higher than 30 ºC, as is the case of heat producing waste, the primary defects are very mobile due to thermal diffusion (Hodgson *et al.*, 1979). The H-centres are easily trapped in the vicinity of dislocation lines, where molecular chlorine is

formed. In addition, the F-centres can react with Na^+ to form metallic sodium. These metallic sodium atoms tend to form clusters of colloidal size (known as colloidal sodium).

Gamma irradiation also causes decomposition of the organic matter present in the rock salt and radiolysis of brine, which leads to the formation of H_2, H_2O_2 and ClO^- species (Jenks *et al.*, 1975).

The importance of the study of radiolytical gas formation is justified by its impact on the operational phase of the storage facility and on the long term safety. The main effects to be taken into account are: pressure build up in the repository, formation of a corrosive atmosphere, generation of explosive and toxic gas mixtures, and changes in the Eh/pH of brines.

The work reported here is complementary to other studies carried out by other partners (ANDRA and GSF) of the HAW project. (Palut *et al.*, 1993; Jockwer, in press)

2. EXPERIMENTAL PROCEDURES

The starting material for the irradiation experiments is natural rock salt from the Potasas del Llobregat Mine. Before the irradiation experiments, the water content and the chemical composition were analyzed.

The water content of the starting material was determined by thermogravimetry, and the mineralogical composition was quantified from chemical analysis. Chlorides were determined volumetrically (Mohr method), sulphates determined by ICP-AES (inductively coupled plasma atomic emission spectrometry), and the insoluble fraction calculated gravimetrically (Huertas *et al.*, 1992). In order to determine the amount of organic matter, Total Organic Carbon (TOC) measurements were perfomed in a TOC analyzer (dilution 1:3000). Quantification was performed through peak area integration using the external standard method (the standard concentrations ranged between 2 and 5 ppm of potassium hydrogen phthalate).

The effect of the generation of radiolytical gases was tested in pure and impure rock salt. Crushed salt samples (125g, size < 1 cm), were placed in borosilicate ampoules using natural air as atmosphere, which were then sealed. The volume ratio between salt and air equaled 1. In order to determine the effect of irradiation on the brine, 200 ml of synthetic brine representative of the starting material (Na 2.91 M, Mg 1.15 M, K 0.31 M, SO_4 0.07 M

and Cl 5.40 M) was also placed in two ampoules. One ampoule of air was also irradiated to be used as blank.

Since most gamma radiation energy is converted into heat, two sets of experiments were performed. Duplicate samples were used in both sets of experiments in order to discern which gases were due to the thermal effect and which to radiolysis. The first set of experiments consisted of two laboratory degasification tests carried out in an oven at a constant temperature of 50°C. The first test took 17 hours and the second took 34 hours. The second set of experiments consisted of two irradiations performed in the industrial irradiator CESAR located at Granollers (Spain). This facility operates with Co^{60} sources. In the first irradiation experiment (17 hours) samples received a total dose of 500 kGy, and in the second (34 hours) the dose was 1 MGy . The irradiation conditions for both experiments were: dose rate about 30 KGy/h and temperature from 20° up to 50°C.

Gases were analyzed by gas chromatography (H_2, CO_2, O_2 and light hydrocarbons) and ion chromatography (chlorine-bearing, NO_x and SO_x gases). H_2, CO_2, O_2 and hydrocarbons were quantified by gas chromatography through peak area integration using the external standard method. Samples and standards were injected repeatedly until less than 5% dispersion in the area measurement was observed. The analytical conditions were:

For H_2 and O_2 analysis: Molecular Sieve 5A 80/100 mesh, 3m 1/8" OD; 60°C hold; Carrier gas: Ar, Detector: Thermal Conductivity (TCD).
For CO_2 and light hydrocarbons analysis: Porapak Q 50/80 mesh, 4m 1/4" OD; 120°C hold; Carrier gas: He, Detector: Thermal Conductivity (TCD).

Gas determination by ion chromatography was carried out after dissolving 10 ml of gas sample in 2 ml of a basic aqueous solution (1 mM NaOH). Ionic species were quantified through IC profiles using the external standard method (the standard concentrations ranged between 0.5 and 10 ppm of Cl^-, SO_4^{2-}, NO_2^- and NO_3^-).

In order to determine whether chlorine-bearing gases were trapped in the rock salt, samples were ring milled, and a gas sample was extracted through a septum placed on the mill lid. In addition, the amount of colloidal sodium was determined in order to check the mass balances between chlorine-bearing gases and colloidal sodium. Colloidal sodium was quantified by monitoring the release of H_2, after dissolution of 150 mg of irradiated rock salt in 1.5 ml double-distilled water. The reaction, which is shown in equation [1], took place in a glass vial (V= 5 ml) which was closed with an open-hole screw-cap and a septum. The analysis of H_2 was performed as described above.

$$Na^o + H_20 \longrightarrow 1/2\ H_2 + NaOH \qquad [1]$$

The pH of the brines was measured by a combined glass electrode, and the redox potential of the brines was monitored by means of a platinum wire using that of the combined glass electrodes as a reference (Casas *et al.*, 1992).

3. RESULTS

The results of the geochemical characterization of the studied rock salt are listed in Table 1. These samples were used as starting material for the thermal degasification and radiolytical gas production experiments.

3.1 Thermally induced degasification of rock salt

The gases released by thermal degasification are listed in Table 2. The results show that besides O_2 (present in the gas atmosphere during the test), CO_2 and CH_4 are also present. Similar results were found in other degasification tests performed in the same rock salt formation (see article 8 of this volume).

The amount of CO_2 is not time dependent, suggesting that its desorption takes place during the first few hours after heating. Impure rock salt contains slightly higher amounts of CO_2 than pure rock salt.

The presence of CH_4 is also associated with the impure rock salt. A relationship between the measured amounts of CH_4 and the potential amount of thermally releaseable gases (mainly CH_4) arising from the decomposition of the organic matter present in the rock, is not apparent. The low contents of measured CH_4 suggests that thermal decomposition of the organic matter has not still taken place at this temperature. Moreover, the desorption of CH_4 is not time dependent since it took place at the early stages of the experiment. The presence of H_2, when compared with results of previous experiments (see article 8 in this volume), could be explained by the fact that the concentration in the gas phase was increased by lowering the volumetric ratio between atmosphere and rock salt sample.

Table 1: Chemical composition of Potasas del Llobregat samples used in the degasification experiments.

SAMPLE	HALITE %	ANHYDRITE %	CLAY %	IG. BRINE %	F.I %	TOC ppm
11	98.32	1.66	0.12	0.12	0.14	43
12	98.61	1.20	0.19	0.09	0.07	105
41	87.44	11.94	0.64	0.23	0.15	122
42	98.90	1.02	0.08	0.06	0.29	78

Note: IG.brine stands for intergranular brine, F.I for fluid inclusions and TOC for total organic carbon content.

Table 2: Thermally induced (50°C) degasification experiment.

SAMPLE	HEATING PERIOD hours	H_2 µg/kg	CO_2 mg/kg	O_2 ml/l	CH_4 mg/kg	NO_x ml/l	SO_x mg/kg
11	17	13	3.6	55	tr	n.d	n.d
11	34	9	3.7	64	n.d	n.d	n.d
12	17	tr	1.4	59	n.d	n.d	n.d
12	34	32	4.4	61	n.d	n.d	n.d
41	17	70	4.3	61	0.2	n.d	n.d
41	34	21	4.1	62	tr	n.d	n.d
42	17	7	3.7	61	n.d	n.d	n.d
42	34	38	3.7	65	n.d	n.d	n.d

Note: Gas content of H_2, CO_2 and SO_x are expressed as mg or µg per kg rock salt. Gas content of O_2 and NO_x are expressed as ml/litre in the gas phase.; n.d = not detected; tr = trace (about 1 µg/kg in the case of H_2 and 10 µg/kg in the case of CH_4).

Table 3: Laboratory degasification experiment of samples subjected to heat (50°C) and gamma radiation.

SAMPLE	DOSE kGy	H_2 µg/kg	CO_2 mg/kg	O_2 ml/l	Cl mg/kg	NO_x µl/l	SO_x mg/kg
11	500	33	3.4	57	---	---	---
11	1000	45	4.6	44	2.2	0.4	1.96
12	500	63	4.1	44	0.6	0.8	0.31
12	1000	60	5.2	56	2.2	2.4	0.80
41	500	145	3.8	56	---	---	---
41	1000	157	4.9	34	1.2	1.4	0.61
42	500	47	3.2	33	0.4	tr	0.45
42	1000	23	5.1	59	0.9	0.4	1.90
BRINE	500	4000	1.2	52	---	---	---
BRINE	1000	5700	---	48	0.04	1.3	0.35
AIR	1000	5	1.1	48	---	---	---

Note: Gas content of H_2, CO_2, Cl and SO_x in rock salt samples are expressed as mg or µg per kg, whereas in brine and air are expressed as mg or µg per litre brine or air respectively. Gas content of O_2 and NO_x are expressed as ml or µl per litre in the gas phase. --- = not analyzed.

Table 4: Comparison between the measured and calculated $G(H_2)$ values.

SAMPLE	DOSE kGy	H_2 µg/kg	IG %	G meas.	G calc.
11	500	33	0.12	0.0140	0.0011
11	1000	45	0.12	0.0098	0.0008
12	500	63	0.19	0.0202	0.0017
12	1000	60	0.19	0.0153	0.0012
41	500	145	0.23	0.0428	0.0021
41	1000	157	0.23	0.0336	0.0015
42	500	47	0.06	0.0061	0.0005
42	1000	23	0.06	0.0049	0.0004

Note: H_2 values expressed as µg H_2 for Kg rock salt and IG stands for intergranular brine and is expressed in % weight. G meas. stands for measured $G(H_2)$ value, whereas G calc. stands for calculated $G(H_2)$ value. The calculated $G(H_2)$ value is computed by multiplying the amount of intergranular brine by the experimental $G(H_2)$ values for brines. $G(H_2)$ value for a dose of 500 kGy equals 0.92, whereas $G(H_2)$ value for a dose of 1 MGy equals 0.65.

3.2 Gas generation due to the combined effect of heat and gamma radiation on rock salt

The gases released in the irradiation experiments are listed in Table 3. It is noticeable that CO_2 increases with irradiation time. Nevertheless, most of the CO_2 released is related to thermal desorption, and only minor amounts are attributable to radiolysis. CH_4 was not detected in samples that had been subjected to radiolysis, in contrast to their equivalents that were subjected to heating experiments. The absence of CH_4 in the irradiated samples could be explained by reaction with O_2, which would produce CO_2 and H_2 under gamma ray exposure, as proposed by Bonne *et al.* (1980) in equivalent experiments in Boom clay samples, which are enriched in hydrocarbons.

The radiolytic yield (G) for H_2 production arising from the radiolysis of water and brines has been extensively studied in a variety of experimental conditions (Brewitz and Mönig, 1992; De Canniere *et al.*, 1992). The G-value is the number of gas molecules generated per 100 eV. The G-values for H_2 production in irradiated brines vary between 0.45 and 2.1 (Brewitz and Mönig, 1992), whereas in aqueous-like solutions (De Canniere *et al.*, 1992) they range between 0.65 (for a dose of 210 kGy) to 0.25 (for a dose of 13500 kGy). The G-values obtained for the brines studied in our experiments are 0.92 for a dose of 500 kGy and 0.65 for a dose of 1 MGy. The G-values obtained empirically in the studied salt samples and those expected taking into account their intergranular water content, are given in Table 4. The measured G-values are higher than the expected, suggesting that part of the H_2 is from other sources.

While the radiolysis of brines has been studied extensively, the multicomponent system reactions of the gas phase are not so clear. The production of CO_2 and H_2 from the recombination of CH_4 and O_2, cannot be explained from the obtained results. An additional source of CH_4 may be involved, which could be the degradation of the organic matter induced by irradiation. Moreover, there is a depletion of O_2 in some of the samples, which supports the hypothesis that CH_4 can be generated when sufficient organic matter is present in the rock salt under oxidizing conditions.

The production of H_2 depends on dose and, as pointed out above, on the amount of water, organic matter and CH_4 present in the rock salt. NO_x is an irradiation product of air (Palut et al, 1993) which increases with increasing dose. The amount of chlorine-bearing gases (probably Cl_2 and $HCl_{(g)}$; Brewitz and Mönig, 1992) increases with dose and is of the same order of magnitude as the amount of colloidal sodium. The amount of SO_x also increases with the dose, which cannot be explained yet, since it is not related to the amount of

sulphatic minerals present in the rock salt.

The effect of irradiation on the brine has also been studied, since changes in brine properties (Eh and pH among other parameter) affect either the UO_2 or the glass matrices dissolution rate (Grambow, 1990). The initial conditions of the brine, in the presence of air before irradiation, were pH 6.0 and Eh 530 mV. After irradiation, the pH and Eh dropped to 5.6 and to 310 mV and to 4.2 and 430 mV for 500 kGy and 1 MGy respectively. This change of Eh and pH can be relevant, since acidic and oxidizing conditions enhance the liberation of radionuclides.

The amount of colloidal sodium ranges between 3.5 and 4.9 * 10^{-6} mol for a dose of 500 kGy and between 5.7 and 6.8 * 10^{-6} mol for a dose of 1 MGy. Assuming that chlorine-bearing gases are present in form of Cl_2, the molar fractions obtained would range between 6.1 * 10^{-7} and 1.0 *10^{-6} mol for a dose of 500 kGy and between 1.4 and 3.6 * 10^{-6} mol for a dose of 1 MGy. The $Cl_2/2Na^o$ ratio in the studied samples was always below 0.2, suggesting that important amounts of Cl_2 may be produced but trapped inside the halite crystals. In order to verify this hypothesis, chlorine-bearing gases present in the irradiated rock salt were determined. Their concentration in the rock salt ranged between 4.6 and 9.8 * 10^{-6} mol (for a dose of 1 MGy), which represent between 60 and 70 % of the produced chlorine-bearing gases. These results confirm that the major part of chlorine-bearing gases are trapped in the rock salt.

4. CONCLUSIONS

Since in irradiation experiments rock salt is subjected to the combined effect of heat and gamma radiation, the key to understanding the generation of radiolytic gases lies in performing duplicate experiments in the same samples subjected only to heat. The experiments reported here, have allowed us to recognize the gases released thermally and those which arise from the direct radiolysis of brine, mineral phases and organic matter present in the rock salt studied. Moreover, it has been shown that a third source of gas production is related to complex interactions of the multicomponent system of the gas phase.

Regarding the gases released by heating, besides the presence of oxygen attributed to the use of natural air as atmosphere in the experiments, degasification of rock salt leads to influx of CO_2, and minor contents of CH_4 and H_2 to the gas phase. There is a relationship between the mineralogical composition of the rock salt and the amount of CO_2 and CH_4. On the other hand no relationship was found between the amount of CH_4 and the amount of

organic matter contained in the sample. This observation supports the hypothesis that thermal decomposition of the organic matter takes place at temperatures higher than 50°C.

In the case of the degasification of rock salt subjected to heat and gamma radiation, the production of CO_2, H_2, NO_x, chlorine-bearing gases and SO_x increases with the dose absorbed. However, CH_4 is absent and the amount of O_2 is lower in some of the irradiated and heated sample than in only heated samples. The relationship between mineralogical composition of the rock salt and gas yields, which was found in the experiments where the samples were only heated, cannot be extrapolated to the samples subjected to the combined effect of heat and gamma radiation experiments.

NO_x is an irradiation product of air, whereas the presence of SO_x is not fully understood. The amount of chlorine-bearing gases is of the same order of magnitude as the concentration of colloidal sodium. However, the ratio $Cl_2/2Na^o$ is below 0.2, which suggests that part of the Cl_2 is trapped in the halite crystals. The trapping of chlorine-bearing gases in the NaCl lattice has furthermore been confirmed by gas analysis of ground rock salt, where the additional chlorine-bearing gases (ratio about 0.6) make the $Cl_2/2Na^o$ closer to 1. This phenomenon would minimize the output of chlorine-bearing gases through the repository.

Besides the production of H_2 due to radiolysis of H_2O, minor amounts of chlorine-bearing gases are formed in the brine radiolysis experiments. Furthermore, the hypothetical presence of oxidizing species in solution such as H_2O_2 and ClO^- could be responsible for Eh and pH changes in the brine. The initial conditions of pH of 6.0 and Eh of 530 mV dropped to 5.6 and to 310 mV and to 4.2 and 430 mV for 500 kGy and 1 MGy respectively. This change of Eh and pH of the brine due to radiolysis can be relevant, since acidic and oxidizing conditions enhance the liberation of radionuclides.

Comparison of both sets of experiments (not irradiated and irradiated) suggests that irradiation favours the production of CO_2 and H_2 from the recombination of CH_4 with O_2. However, the results indicate that not all the CO_2 and H_2 can be attributed to the combined action of direct radiolysis of the brine and radiolytic oxidation of CH_4. It is therefore inferred that an additional source of CH_4 might have been present, which probably consisted of the organic matter present in the samples.

The obtained results show that small amounts of corrosive, toxic and explosive gases will be formed by heating and/or gamma irradiation of rock salt. The amount of the gases produced by irradiation (NO_x, SO_x, H_2 and chlorine-bearing gases) will depend on dose and temperature, and probably will affect only the engineering barrier made of salt backfill.

Moreover, brine will become more acidic and oxidized, enhancing the liberation of radionuclides. Furthermore, the amount of gases derived from thermal degasification (mainly CO_2 and CH_4) is not time dependent and may reach its saturation level at early stages of waste emplacement. Finally, the effect of pressure build-up due to the presence of gases of all origins (overpressure in the glass container was noticed after the experiments), could be minimized by proper design of long-term seals in the repository concept.

ACKNOWLEDGEMENTS

The work reported here has been performed on behalf of ENRESA under contract No 70.2.3.13.03. We are indebted to Mr. J.M. Grosso from the LIFS for the chemical analyses and to Ms. R.M. Marimon and Ms. L. Balart from the Serveis Cientifico-Técnics de la Universitat de Barcelona (U.B) for the I.C. and T.O.C. analyses. We also wish to thank Ms. M.E. Torrero of the Dept. d' Enginyería Química de la Universitat Politècnica de Catalunya (UPC), who kindly performed the Eh/pH measurements in brines.

5. REFERENCES

BONNE, A., HEREMANS, R., and VANDERBERGHE, N, 1980: *"Possibility of disposing of conditioned nuclear waste in deep lying clay formations"* in "Proceedings of the Symposium on Geology and Nuclear waste disposal", Utrecht, Geol. Ultraiectina, Spec. Publ. nº 1, 377-392

BREWITZ. W, and MÖNIG, J., 1992: *"Sources and migration pathways of gases in rock salt with respect to high level waste disposal"* in "Proceedings of the Workshop on Gas generation and release from radioactive waste repositories", Aix-en-Provence, NEA-OCDE, 41-53

CASAS, I., DE PABLO, J., GIMENEZ, J., TORRERO, M.E., and AGUILAR, M., 1992: *"Solubility studies of Uranium dioxide under the conditions expected in a saline repository. Phase II"*, ENRESA Publicación Técnica 05/92, 51p

DE CANNIERE, P. HENRION, P. VAN ISEGHEM, P. and VOLCKAERT, G., 1992: *"Radiolytic gas generation and H2 reaction experiments at SCK/CEN (Mol)"* in "Proceedings of the Workshop on Gas generation and release from radioactive waste repositories", Aix-en-Provence, NEA-OCDE, 202-203

GRAMBOW, B., 1990: *"Status in understanding and modelling radionuclide release from high level waste glass and spent fuel"* in "Proceedings of the Int. Symp. on the Safety Assessment of radioactive waste repositories", Paris, NEA-OCDE, 439-458.

HODGSON, E.R., DELGADO, G. and ALVAREZ RIVAS, J.L., 1979: *"In-beam studies of M-centre production processes in NaCl"*, Jour.Phys. C: Sol.Sta.Phys., **12**, 1239-1244

HUERTAS, F., MAYOR, J.C., and DEL OLMO, C., 1992: *"Textural and Fluid Phase Analysis of Rock Salt subjected to the combined effects of Pressure, Heat and Gamma Radiation"*, Nuclear Science and Technology, EUR 14169 EN, 218p

JENKS, G.H., SONDER, E., BOPP, C.D., WALTON, J.R. and LINDEBAUM, S., 1975: *"Reaction products and stored energy released from irradiated sodium chloride by dissolution and by heating"* Jour. Phys. Chem., **79**, 871-875

JOCKWER, N., in press: *"Irradiation of salt samples at the HFR in Petten"* in "B. Haijtink and T. McMenamin (Eds) Project on effect of gas in underground storage facilities for radioactive waste", Nuclear Science and Technology, EUR series

PALUT, J.M., GAUDEZ, M.T. and AKRAM,N., 1993: *"Gas generation by radiolysis of rock salt -HAW PROJECT-"* in "B. Haijtink and T. McMenamin (Eds) Project on effect of gas in underground storage facilities for radioactive waste", Nuclear Science and Technology, EUR 14816, 65-80

GAMMA-RADIOLYTIC GAS PRODUCTION IN GROUND ROCK SALT OF HOMOGENEOUS COMPOSITION

N. Jockwer, H. Sprenger, K.-H. Feddersen, J. Mönig

ABSTRACT

Natural rock salt samples, that are representative for a repository in the salt diapirs in northern Germany, have been γ-irradiated at the High Flux Reactor (HFR) at Petten, The Netherlands, using spent fuel elements. The γ-radiolytic formation and release of gases was studied by gas chromatography. Radiation doses varied between 10^6 and 10^8 Gy, while the effect of temperature was investigated between 100 and 250 °C. The gas atmosphere in which the rock salt is irradiated has a significant influence on the product composition. When the irradiations were carried out in synthetic air, N_2O, CO, CO_2, as well as some H_2 were detected. Under a helium atmosphere H_2, CH_4, and CO_2 were observed as gaseous products, while no CO or N_2O was detected. From our data, it is concluded that the contribution of the γ-radiation-induced gas formation to the total source term of gas production in an emplacement borehole for vitrified high level radioactive waste should be negligible. Other processes such as the formation of hydrogen via corrosion and the pressure increase due the creeping of the salt are much more important for the safety considerations.

1. INTRODUCTION

The emplacement of canisters containing vitrified reprocessed high level radioactive waste in boreholes in rock salt will result in an exposure of the host rock to temperatures up to 200 °C and gamma dose rates of 1000 Gy. The total dose in a repository is estimated to be in the order of 10^9 Gy. Apart from the development of radiation damage in rock salt, γ-radiation leads to the formation and release of gases from the rock salt. The processes of gas formation are of interest as they may lead to a pressure build-up, and to the formation of explosive and/or corrosive gas mixtures in sealed repository areas [Brewitz and Mönig, 1992]. Gases may also provide a means of transportation for radioactive nuclides.

In order to be able to design repositories and to assess their long-term safety, it is necessary that all sources contributing to the generation and release of gases are known qualitatively and quantitatively. Several different processes account for the gas generation and contribute to the total source term for gas production in the emplacement of high level radioactive waste. These include the gas release from the rock salt at ambient and elevated temperatures, the gas generation from the emplaced waste, e.g. via corrosion of the waste canisters, and the radiation-induced gas generation. The extent to which each of these processes contributes to the total gas generation rate depends on various factors, i.e. the waste type, the host rock and the specific disposal conditions.

The question of γ-radiation-induced gas formation and release from rock salt was addressed in some detail in previous studies [Jockwer, 1983, Jockwer and Gross, 1985, Jockwer and Mönig, 1989]. It was also the subject of another irradiation program, that was carried out in collaboration with ANDRA and CEA-SACLAY [see articles 5 and 14, this volume]. The present irradiations were meant to determine the radiation damage in natural rock salt samples from the Asse salt mine (Remlingen, Germany) [Mönig et al., 1995 (article 16, this volume)]. However, since these irradiations were carried out in sealed glass ampoules, it seemed worthwhile also to measure the radiation-induced gas formation and release in these samples for comparison with previous data. Here we report on these results. The experimental methodologies are described in detail elsewhere [Mönig et al., 1995 (article nr. 8, this volume)].

2. RESULTS

The gas atmosphere in which the rock salt is irradiated has a significant influence on the product distribution. When the irradiations are carried out in synthetic air, N_2O, CO, CO_2, as well as some H_2 were detected. Under a helium atmosphere H_2, CH_4, and CO_2 were observed as gaseous products, while no CO or N_2O was detected. Other aliphatic hydrocarbons than CH_4 (e.g. C_2H_6) were also found but only in very small quantities (< 0.01 ppm), so that the individual results are not given here. H_2S was not detected in any sample.

The obtained product quantities depend on the absorbed dose and on the temperature. The dose dependence of the various gases at 100°C, 150°C, 200°C, and 250°C are shown in Figs. 1 - 3 for irradiations in helium and in Figs. 4 - 7 for irradiations in synthetic air, respectively. The gas yields are expressed in ppm, i.e. as mg gas per kg rock salt. They were calculated from the measured gas phase concentrations using the ideal gas law as follows:

$$y = \frac{GPV_{total} \cdot GPC \cdot MW}{MV \cdot m_s} \qquad (1)$$

where:

y	= yield [µl/g]
GPC	= measured gas phase concentration [µl/l]
GPV_{total}	= volume of gas phase in total system [l]
MW	= molar weight of gas component [g/mol]
MV	= molar volume of ideal gas at 25 °C (24.465 l/mol)
m_s	= mass of rock salt in the ampoule (300 g)

The data for N_2O are only given in relative units, as no test gas mixture was available for calibration during the experiment. However, the absolute yields can roughly be estimated using the response factors for hydrogen and oxygen, which are also detected on this chromatographic channel, and taking the differences in the heat conductivity of the various gases into account. On this basis a N_2O-yield of 1000 (rel. units) corresponds to a gas phase concentration of about 6 Vol-% N_2O in the glass bulb that was used for the gas measurements.

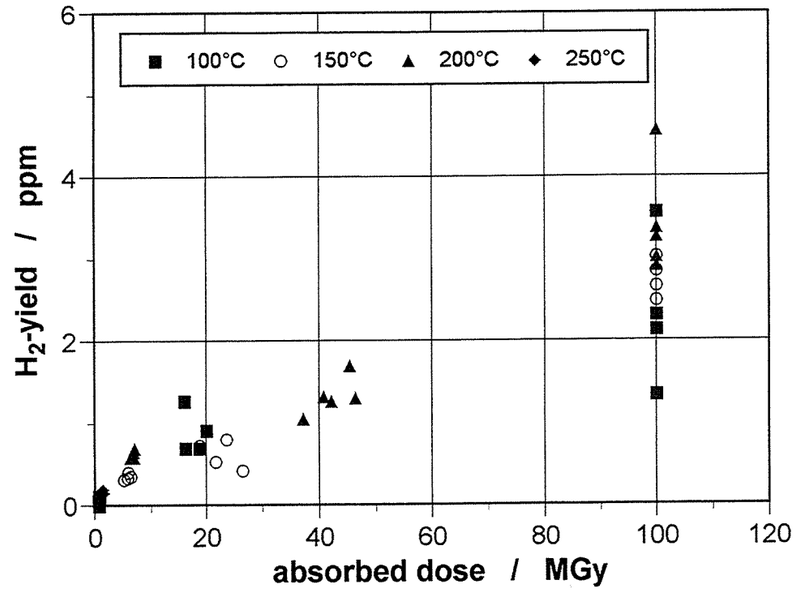

Figure 1: *Yield of hydrogen vs. absorbed dose at various temperatures for γ-irradiated rock salt in a helium atmosphere.*

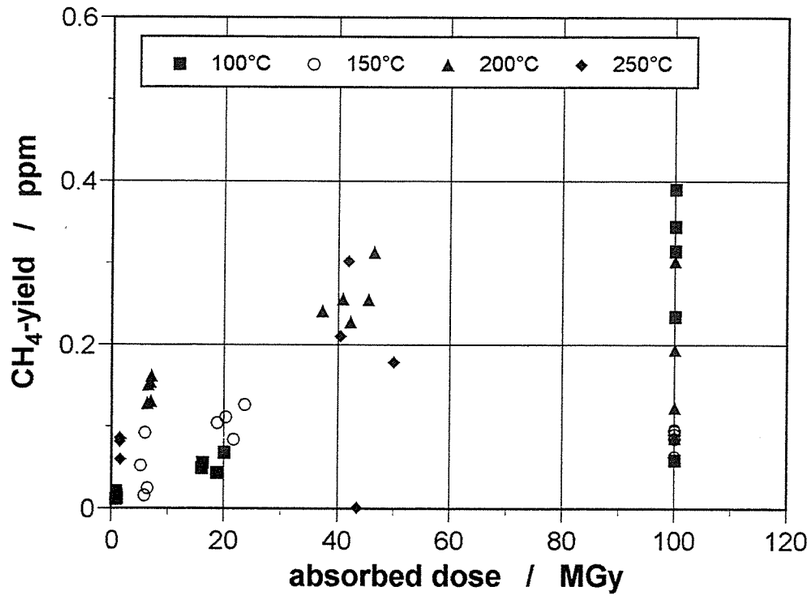

Figure 2: *Yield of methane vs. absorbed dose at various temperatures for γ-irradiated rock salt in a helium atmosphere.*

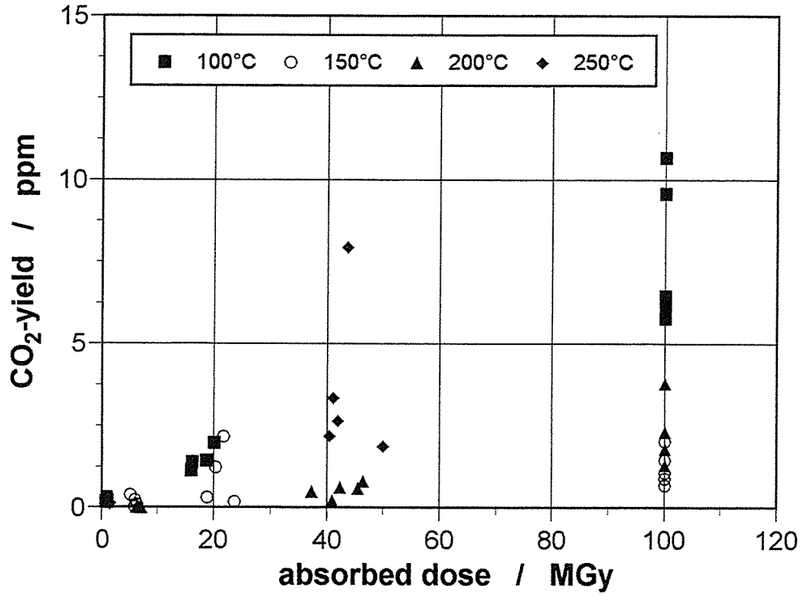

Figure 3: *Yield of carbon dioxide vs. absorbed dose at various temperatures for γ-irradiated rock salt in a helium atmosphere.*

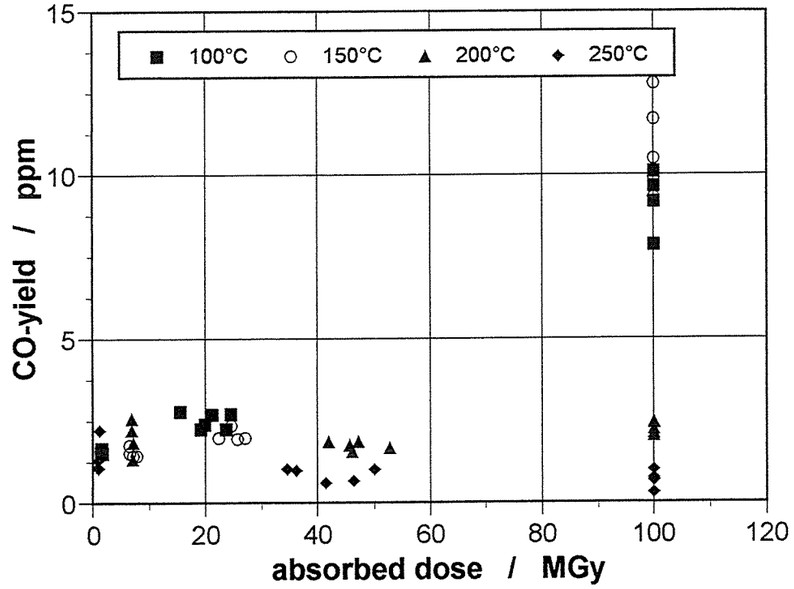

Figure 4: *Yield of carbon monoxide vs. absorbed dose at various temperatures for γ-irradiated rock salt in a synthetic air atmosphere.*

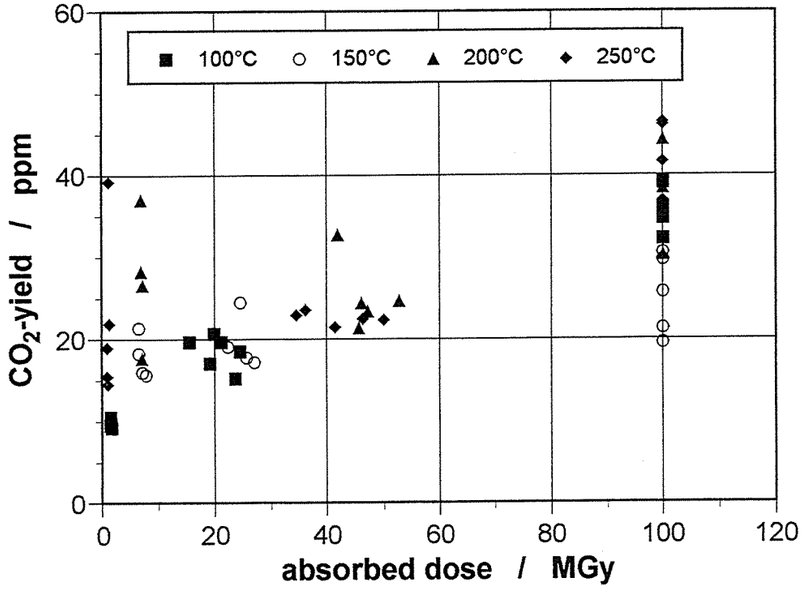

Figure 5: *Yield of carbon dioxide vs. absorbed dose at various temperatures for γ-irradiated of rock salt in a synthetic air atmosphere.*

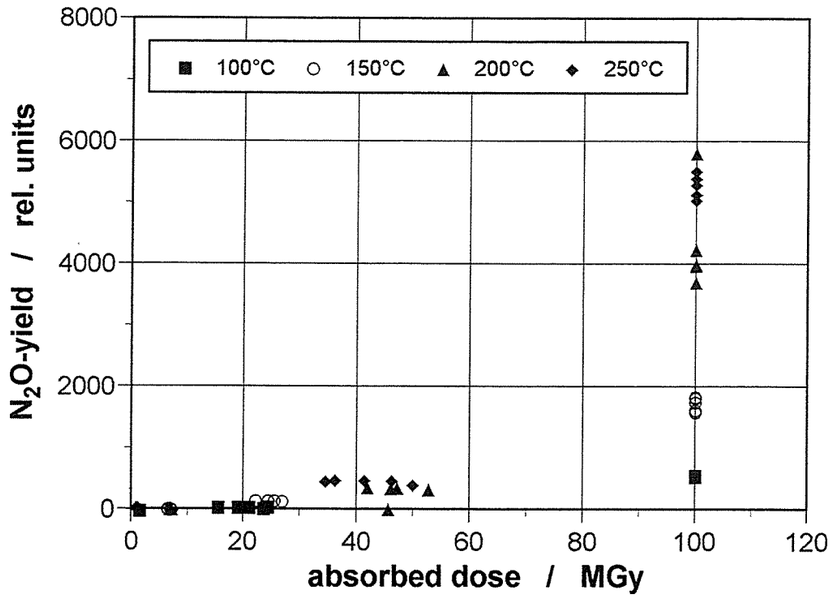

Figure 6: *Yield of dinitrogen oxide vs. absorbed dose at various temperatures for γ-irradiated rock salt in a synthetic air atmosphere.*

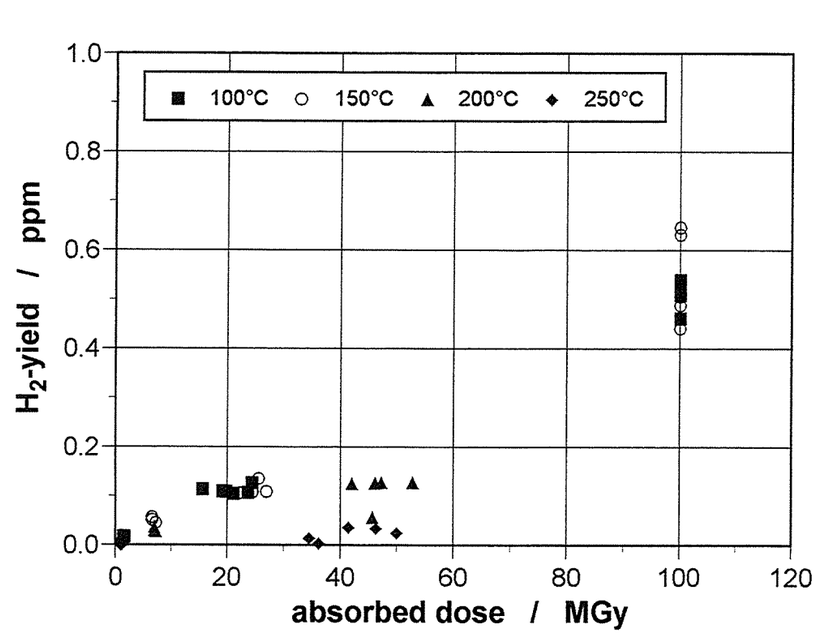

Figure 7: *Yield of hydrogen vs. absorbed dose at various temperatures for γ-irradiated rock salt in a synthetic air atmosphere.*

3. DISCUSSION

Figures 1 - 3 reveal, that the gas yields depend on radiation dose but only slightly on temperature, when the irradiations are carried out under a helium atmosphere. The generation of hydrogen increases almost linearly with increasing dose, while the CH_4- and CO_2-yield seem to level off at the highest doses. The hydrogen is produced by radiolytic decomposition of water. This process occurs either homogeneously in the gas phase or heterogeneously on the salt surface.

In the presence of oxygen, the hydrogen yield is considerably reduced (Fig. 7). This applies generally to all temperatures and radiation doses. In contrast to irradiations in helium, the hydrogen yields in an oxygen atmosphere show a marked dependence on temperature. Hardly any hydrogen is found at 200 °C and 250 °C. As outlined above, hydrogen is formed by two processes. In the homogeneous gas phase reaction hydrogen is produced via the bimolecular reaction of two hydrogen atoms, that are produced by radiolytic decomposition of water molecules in the gas phase.

$$H_2O \rightarrow {}^{\bullet}OH + H^{\bullet} \qquad [1]$$

$$H^{\bullet} + H^{\bullet} \rightarrow H_2 \qquad [2]$$

In the presence of oxygen, the hydrogen atoms react exclusively with oxygen (reaction **[3]**), as the steady state concentration of hydrogen atoms in the gas phase is orders of magnitude lower than that of O_2. The resulting $HO_2^{\bullet}$ radical reacts further, but does not produce H_2.

$$H^{\bullet} + O_2 \rightarrow HO_2^{\bullet} \qquad [3]$$

The data shown in Figs. 1 and 7 suggest that also a heterogeneous reaction forming hydrogen occurs at the rock salt. In this reaction, water molecule adsorbed at the surface are radiolytically decomposed similar to reaction **[1]**. However, since this reaction occurs on the salt surface the resulting $H^{\bullet}$ atoms are believed to be stabilized on the solid, thus allowing the combination of two such hydrogen atoms (as in reaction **[2]**). Owing to the dipolar character of the crystal surface, always more water molecules than oxygen molecules should be adsorbed. It follows, that on the salt surface reaction **[3]** can not effectively compete with reaction **[2]**. The H_2-yield in the presence of oxygen, therefore, can be attributed to the

combination reaction of two hydrogen atoms on the surface of the salt crystal. At the higher temperatures low H_2-yields are observed since under these conditions hardly any water is adsorbed at the crystal surface.

Carbon dioxide were found both when irradiations were performed under helium and under air. In a helium atmosphere carbon dioxide is not produced by radiolytic processes. Its appearance in the gas phase is attributed to desorption from the rock salt surface. The same applies to methane. However, both yields are fairly low and exhibit some scatter. In control experiments in which ampoules were exposed to various temperatures but not irradiated, both carbon dioxide and methane were also detected (data not shown). The data in Figs. 2 and 3 suggest an upper yield of about 7 ppm CO_2 and of 0.3 ppm CH_4 per gram salt, respectively.

Desorption from the salt surface depends surely on time. It is expected that desorption will also depend on temperature. Therefore, desorption of CH_4 and CO_2 should occur considerably faster at the higher temperatures and the upper yields should be reached in shorter times, i.e. at lower doses. However, such a dependence is not apparent in Figs. 2 and 3. Quite in contrast, the highest CO_2-yield is obtained at the lowest temperature. It is possible that the release of the gases is facilitated by radiation damage of the crystal lattice. This kind of synergistic effect has been observed previously [Jockwer and Mönig, 1989]. Since the extent of radiation damage is much higher at 100°C than at 200°C, it could outweigh the temperature effect on desorption.

In the presence of oxygen during the irradiation, methane and other hydrocarbons are radiolytically oxidized forming CO and CO_2. Thus, no methane is found in these systems and the CO_2-yield is about fivefold higher than in oxygen-free systems. Some carbon dioxide could also originate from thermal oxidation of hydrocarbons. The data indicate a small temperature dependence for the formation of CO and CO_2. The higher the temperature, the lower the CO-yield while the respective CO_2-yield increases.

N_2O is formed from nitrogen and oxygen via gas phase reactions. The yield clearly increases with temperature. Interestingly, such a strong variation with temperature was not observed by Akram et al. [Akram et al., 1992]. The reaction scheme for the gas phase radiolysis of moist air is very complex [Reed and Konynenburg, 1988]. A variety of products are formed, other products besides N_2O include nitrous oxide, nitric acid and so on. These products have not been determined in the frame of our investigation. The relative yields of the various products depend very strongly on the boundary conditions of the experiment.

From our data, one can estimate the order of magnitude for the radiation-induced gas production that would occur in a repository with disposal of vitrified high level waste in boreholes. Approximately 25 cm of salt around the borehole are affected by radiation. Assuming a borehole diameter of 60 cm, one can estimate the following numbers for the gas production per meter borehole at 10^8 Gy.

Table 1: *Estimated gas production in an emplacement borehole for vitrified high-level waste at 10^8 Gy (assuming a borehole diameter of 60 cm and a zone of 25 cm rock salt around the borehole that is affected by radiation)*

gas component	gas production (in l) per meter borehole at 10^8 Gy
H_2 (in oxygen-free environment)	60.0 l/m
CH_4 (in oxygen-free environment)	0.7 l/m
CO_2 (in air)	30.0 l/m

A borehole with a diameter of 0.60 m has a volume of about 280 l per meter length. At 10^8 Gy the gas production both in the presence of air and in its absence totals less than 100 l. Therefore, only a small pressure increase due to the radiation-induced gas formation should occur. The contribution of this process to the total source term is apparently very low. In aerated systems nitrogen and oxygen are converted into N_2O, but this process also does not lead to a pressure increase. The gas production via other processes such as the formation of hydrogen via corrosion and the pressure increase due the creeping of the salt are much more important for the safety considerations.

REFERENCES

N. AKRAM, M.T. GAUDEZ, P. TOULHOAT, J. MÖNIG, J.M. PALUT, 1992: "*Multi-Parameter Study of Gas Generation Induced By Radiolysis of Rocksalt in Radioactive Waste Repositories*" in "Gas Generation and Release from Radioactive Waste Repositories", Proc. NEA-Workshop, Aix-en-Provence, 23-26 Sep. 1991, OECD, 130 - 141

W. BREWITZ and J. MÖNIG, 1992: "*Sources and Migration Pathways of Gases in Rock Salt with Respect to High Level Waste Disposal*", in "Gas Generation and Release from Radioactive Waste Repositories", Proc. NEA-Workshop, Aix-en-Provence, 23-26 Sep. 1991, OECD, 41 - 53

N. JOCKWER, 1983: "*Laboratory Investigations on Radiolysis Effects on Rock Salt with Regard to the Disposal of High-Level Radioactive Wastes*", in "Scientific Basis for Nuclear Waste Management VII", Ed.: G.L. McVay, Mater. Res. Soc. Proc. **40**, USA, 17 - 25

N. JOCKWER and S. GROSS, 1985: "*Natural, Thermal and Radiolytical Gas Liberation in Rock Salt as a a Result of Disposed High-Level Radioacive Waste*", in "Scientific Basis for Nuclear Waste Management IX", Ed.: L.W. Werne, Mater. Res. Soc. Proc. **50**, USA, 587 - 594

N. JOCKWER and J. MÖNIG, 1989: "*Laboratory Investigation into the Radiolytic Gas Generation from Rock Salt. A Study Related to the Disposal of High Level Radioactive Waste*", in "Scientific Basis for Nuclear Waste Management XII", Eds.: W. Lutze, R.C. Ewing, Mater. Res. Soc. Proc. **127**, USA, 913 - 920

D.T. REED and R.A. VAN KONYNENBURG, 1988: "*Effect of Ionizing Radiation on Moist Air Systems*", in "Scientific Basis for Nuclear Waste Management XI", Eds.: M.J. Apted, R.E. Westerman, Mater. Res. Soc. Proc. **112**, USA, 393 - 404

ANALYSES OF RADIOLYTIC GASES RESULTING FROM GAMMA IRRADIATION OF ASSE ROCKSALT PERFORMED AT SACLAY.

M.T. Gaudez, N. Akram, P. Toulhoat, N. Toulhoat, J.M. Palut

ABSTRACT

The radiolytic generation of gases is an issue which has been considered when studying the safety of radioactive waste repositories in rocksalt. During these 5 years of research over 350 samples of ground salt have been irradiated and analyzed in order to elucidate which are the mechanisms in the radiolytic generation of gases in salt.

We have studied the effect of dose and dose rate at different temperature in the amount and nature of generated gases. The irradiated samples were of different composition and granulometry, in this way different backfill characteristics could be simulated. the samples were encapsulated in glass vials prior to irradiation. The gases contained in the vials were analyzed after irradiation. Samples from the same batch were encapsulated in vials inside which different atmospheres were created. In this way the relationship between original oxidizing, reducing, or inert atmosphere, and the obtained gases could be studied.

The way in which the experiments were performed and the obtained results are here described.

1. INTRODUCTION

ANDRA, the French National Radioactive Waste Management Agency, joined the HAW project in 1988 in the framework of European Community agreements FI1W 0199 and F12W 0002. Andra's involvement relates to calculations, laboratory testing and *in situ* measurements. The objective of laboratory work summarized in this report was parametric study, in a laboratory,

of gas generation by radiolysis of Asse salt. From 1988 to 1993, the test program involved over 350 samples. The first phase of the test protocol developed included preparation of samples and their irradiation at the Saclay Research Center, primarily with spent fuel from the Osiris test reactor. The second phase consisted of analyzing the generated gases by various methods suited to the context of the study : chromatography, mass spectrometry, infrared spectrometry. Test results presented and discussed in this report reveal the preponderance of certain irradiation parameters in gas generation, such as integrated dose, the type of initial gas, salt granulometry and the content of impurities in the salt.

1.1. Purpose of Study

The purpose of the study is qualitative and quantitative assessment of gaseous releases in salt caused by radiation, primarily gamma radiation, emitted by waste canisters. Salt is considered as both the host rock and the principal component of the engineered barriers. The radiation emitted by the waste can induce radiolytic reactions, especially of water or fluids coming from the geologic formation (gases or liquids). These reactions, combined with a temperature rise in the near field, may produce toxic, corrosive or even explosive substances.

Gamma irradiation of salt samples therefore had to be performed under a variety of conditions by varying the essential parameters of the phenomenon studied in realistic areas in terms of disposal and test duration : dose rate, temperature and duration of irradiation, salt granulometry and composition of the atmosphere under which the salt is irradiated. The combination of issues raised also prompted us to look into the material's behavior and damage to the crystalline lattice caused by γ radiation. An understanding of the chemical and mineralogical composition of salt is indispensable in understanding and observing the formation of gaseous compounds.

1.2. Partners

ANDRA cooperated with different CEA teams at the Saclay and Fontenay aux Roses sites in performing these tasks:

- DRN/DRE/SRO for salt irradiation;
- DCC/DSD/SCS to analyze radiolytic gases and process results; and
- DCC/DPE/SPEA for mass spectrometry analyses.

While salt domes are plentiful in Germany, they are rarer in France, where saliferous formations are usually layered. CEA's DCC/DSD/SCS group at Fontenay aux Roses has also carried out work focused specifically on the phenomenology of radiolysis of a French salt from the Mines de Potasse d'Alsace [Akram, 1993].

1.3. Objectives and Planning

The general purpose can be split into some specific experimental objectives which were worked out into a test plan established together with the GSF. Table 1 gives an overview of the parameters which relationships were studied in this program. Carrying out the program meant sample collection and packaging, irradiation of the samples and post irradiation analysis. The irradiation experiments and the methodology of irradiation are described by Marchand (1995, artc. nr. this volume), and will not be repeated here.

The original program as stablished in Table 1 was supplemented with additional studies to better identify the various reactive mechanisms involved, summarized in Table 2.

Previous to carrying out the test plan, during the first half of 1988, two series of irradiations were performed to select sample packaging, sampling procedures and analytical methods suited to the different radiolytic gases. These tests were performed on a 2 kg batch of crushed salt (batch 1) supplied in April 1988 by GSF.

Table 1 : *Asse salt radiolysis : initial programme of irradiations*

Parameter	Number of samples (except blanks)	Dose rate (Gy/h)	Total dose (Gy)	Duration (hours)	Temperature (°C)
Salt cores	9	1. E+4	1. E+6	100	ambient
Crushed salt	15	1. E+4	1. E+6	100	ambient
Grainsize	6 6 6 6 6	1. E+4 1. E+4 1. E+4 1. E+4 1. E+4	1. E+3 1. E+4 1. E+5 1. E+6 1. E+7	0.1 1 10 100 1000	ambient
Dose rate	3 3 3 3	1. E+2 1. E+3 1. E+4 1. E+5	1. E+6 1. E+6 1. E+6 1. E+6	10000 1000 100 10	ambient
Total dose	3 3 3 3 3 3	1. E+3 1. E+3 1. E+3 1. E+3 1. E+3 1. E+3	1. E+2 1. E+3 1. E+4 1. E+5 1. E+6 1. E+7	0.1 1 10 100 1000 10000	ambient
	3 3 3 3 3 3	1. E+4 1. E+4 1. E+4 1. E+4 1. E+4 1. E+4	1. E+3 1. E+4 1. E+5 1. E+6 1. E+7	0.1 1 10 100 1000	
Temperature	3 3 3 3 3	1. E+4 1. E+4 1. E+4 1. E+4 1. E+4	1. E+6 1. E+6 1. E+6 1. E+6 1. E+6	100* 100* 100* 100* 100*	50 100 150 200 250
Pure minerals	21	1. E+4	1. E+6	100	ambient
Containers	15	1. E+3	1. E+6	1000	200
Filling atmos. (N_2, O_2, Ar, He)	12	1. E+4	1. E+6	100	ambient

Table 2 : *Asse salt radiolysis : complementary programme of irradiations*

Parameter	Number of samples (except blanks)	Dose rate (Gy/h)	Total dose (Gy)	Duration (hours)	Temperature (°C)
Dose rate and total dose	3 3	5. E+4 4. E+4	1. E+6 4.9 E+6	20 120	120 80
Crushed salt (with ^{60} Co)	3 3 3	1. E+4 4. E+4 3.3 E+4	1. E+6 2.9 E+6 1.3 E+8	100	ambient 80 65
Massive samples	3	1. E+4	1. E+6	100	ambient
Dose rate, dose and temperature	3 3 3 3 3 3 3 3	1. E+5 1. E+4 1. E+4 1. E+3 1. E+5 1. E+4 1. E+4 1. E+3	1. E+6 1. E+4 1. E+5 1. E+6 1. E+6 1. E+4 1. E+5 1. E+6	10 1 10 1000 10 1 10 1000	150 150 150 150 200 200 200 200
Filling atmos. with increasing O_2 content	3 3 3 3 3 3	1. E+5 1. E+4 1. E+4 1. E+4 1. E+3 1. E+5	1. E+6 1. E+4 1. E+5 1. E+6 1. E+6 1. E+6	10 1 10 100 1000 10	ambient
	3 3 3 3 3	1. E+4 1. E+4 1. E+4 1. E+3 1. E+5	1. E+4 1. E+5 1. E+6 1. E+6 1. E+6	1 10 100 1000 10	

1.4. General Methodology

On the occasion of this research program, we developed an experimental approach which enabled the influence of radiation on gas generation in rock salt to be assessed. This methodology has already been applied to salt samples coming from other sites than the Asse mine, e.g. salts including variable quantities of marl, anhydrite, sylvinite and organic matter. Based on a consistent set of test results, we proposed interpretations in terms of mechanisms,

and initiated predictive modelling of the evolution of the system in a disposal context. This methodology comprises the following points :

- design of the test plan to optimize the parametric area to be explored;
- development of a special irradiator using irradiated or spent fuel supplying a large range of dose rates and integrated doses and providing constant dose rates over several months; optimization of dosimetry on a continuous basis;
- development of procedures for preparation and packaging of samples for irradiation and analysis;
- use of different characterization methods for solid samples, before and after irradiation, some of them being completely new (nuclear microprobe);
- development of various special accurate analytical methods for identification of the gases, particularly chlorides (GPC after chemical reaction) and sulfured products (GPC coupled with mass spectrometry), adaptation of the FTIR to the determination of complex gas mixtures, measurement of certain acidic gases by ion chromatography after trapping, in addition to the conventional methods (GPC and direct mass spectrometry); and
- development of desorption procedures followed by on-line analyses.

2. PRE-IRRADIATION METHODOLOGY.

Salt characterization, especially identification of organic compounds was mainly carried out by microscopic examination. The approach consisted of investigating the medium's characteristics at the moment of geologic formation of the rock, when minerals precipitated. Microscopic inclusions trapped in intracrystalline cavities are representative of original brines. Different techniques, described hereunder, had to be used for qualitative analysis of the medium's different compounds.

2.1. Methodology of the Analysis of Fluids.

Microscopic examination is based on criteria relating to the location, size, form and content of inclusions at ambient temperature. Two types of inclusions may tell the history of the rock: inclusions trapped during the salt deposition, or primary inclusions, and inclusions trapped later, or secondary inclusions.

Microthermometric examination consists of measuring phase change temperatures in an inclusion under a microscope at varying temperature. This gives information on density, overall salinity and the presence of dissolved gases such as CO_2, CH_4 and of other hydrocarbons.

Microthermometry can be combined with other analytical techniques, such as *Raman mol microprobe with laser excitation, Fourier Transform InfraRed microspectroscopy* (FITR), *Electron Spectroscopy* (ESCA) and *nuclear microprobe*.

This latter technique *developed* in the framework of this program is described below.

2.1.1. The Nuclear Microprobe (A New application of the Instrument)

The characterization of the light elements (carbon and oxygen) of the salt was carried out with the nuclear microprobe at CEA's Bruyères le Châtel site. The test device for focusing and analysis is coupled with a 4 MeV Van De Graaff single stage accelerator. Using various spectroscopic modes (elastic diffusion spectrometry, nuclear reactivity analysis, X and γ ray emissions induced by charged particles) information can be gained on three-dimensional elemental and sometimes isotopic distributions of most of the elements in the periodic table. The nuclear microprobe make it possible to do non-destructive elemental characterization of salt samples and to analyze the light element composition of the fluid inclusions.

Experimental Procedure

Nuclear microprobe analysis of salt samples was done by detecting protons and gamma photons emitted during nuclear reactions induced by deuterons. The resulting reactions induced by the deuterons were used to analyze, respectively :

- carbon: $^{12}C(d,p)^{13}C$;
- oxygen: $^{16}O(d,p)^{17}O$ and $^{16}O(d,p\gamma)^{17}O$, $E\gamma = 871$ keV;
- sodium: $^{23}Na(d,p\gamma)^{24}Na$, $E\gamma = 472$ and 1369 keV.

Salt behavior during the irradiations was also observed by analyzing emitted X photons.

The carbon and oxygen content was determined by reference to graphite and silica standards. The salt's contribution to the charged particle spectra was deduced by using (d,α) reactions induced in ^{23}Na and ^{35}Cl. Gamma photon spectra were interpreted taking into account the interferences due to $(n, n'\gamma)$ and $(n,\alpha\gamma)$ reactions induced in the germanium of the gamma detector (energies $E\gamma = 868$ and 875 keV respectively).

Experimental configuration

The following experimental configuration was used :

- deuteron energy: 1.4 MeV;
- microbeam diameter of 25 to 50 μm adjusted to the size of the inclusions;
- current density of 8 to 26 pA/μm^2 inclusive; and
- charged particles and γ and X photons detected by surface barrier detectors (detection angle in relation to incident beam = 120°), Ge HP (angle = 135°) and SiLi (angle = 112°) respectively.

Approximately 2 mm thick sections of salt were polished with alumina powder lubricated with ethylene glycol. A 1/1 solution of dichloromethane/ethanol was used to clean the surfaces. The inclusions analyzed are at a depth of 0 to 15 μm beneath the surface. The polished surfaces were plated with an approximately 30 nm thick gold film to drain off charges and reduce sample damage linked to the temperature increase and ionic erosion at the point of impact.

Verification of salt and inclusion behavior when exposed to an ion beam

The development of F centers and sodium colloids when exposed to an ion beam depends both on the total dose and on the dose rate. For ions of a given type and energy, the density of the current determines the heat applied to the sample during irradiation. Because alkaline halides are particularly sensitive to erosion by electronic sputtering, the use of a high density current that increases the yield of primary defects will also contribute to the diffusion of interstitial halogens towards the surface and vaporization of metal sodium in the surface. The use of a sufficiently low density of current therefore helps to limit the development and diffusion of defects.

The metal-plating film cools the outermost surface and prevents its erosion. In addition this film stabilizes fluid inclusions that have a tendency to migrate along the thermal gradient and, in our case, in the direction of the surface level.

An analysis of signals detected from charged particles and γ and X photons shows 1) no measurable variation in salt composition for current densities of 12 to 15 pA/μm^2 inclusive, and 2) fluid inclusions could be analyzed with a current density of as much as 26 pA/μm^2.

2.2. Methods of Organic Matter Characterization .

The important role played by organic matter during radiolytic reactions prompted us to characterize organic compounds present in the material [GAUDIN and GAUDEZ, 1993].

Some organic compounds present in the material were identified and estimated by chromatographic analysis coupled with mass spectrometric detection. The organic matter was extracted from the salt with dichloromethane.

Silylation of a fraction of the sample by the BSA helped to identify non-soluble products, such as alcohols and acids. These compounds, which are principally linear or branched hydrocarbons and organic acids, are present in very low concentrations ($<10^{-7}$ g/g) in the Asse salt. Examination of the unidentified insoluble fraction in the dichloromethane suggests the

presence of heavier hydrocarbons. The behavior of these products under γ irradiation may lead to the formation of toxic compounds by reaction with the principal constituent (NaCl), giving rise to the formation of chlorinated compounds. The research begun as part of this program together with conclusions pertaining to unhomogeneous saline materials (MDPA) revealed the importance of organic matter during irradiation and will require appropriate analytical development during later work.

2.3. Starting Material (Sample Supply)

The test plan required different types of sample composition and granulometries which were supplied by the GSF as the project progressed and are listed below. The methodology used to produce the samples of natural rocksalt of homogenous composition is extensively described in Gies (1995), art. Nr.. This volume. The samples were prepared from ground Asse rocksalt samples, or constituted by container wall material pieces. The following samples were used:

- 2 kg of crushed salt for preliminary tests (batch 1) ;
- 50 kg of crushed salt (batch 1988) for the irradiation program ;
- five samples of granulometries ranging from 0.125 to 8.0 mm ;
- 2 batches of granulometries in the ranges of ($0.1 < \phi < 0.25$ mm) and ($1.0 < \phi < 2.0$ mm) to study the influence of grain size as a function of integrated dose;
- core drilled samples measuring 20, 30 and 50 mm in diameter and 50 mm high;
- the principal mineralogical compounds of the salt in the form of pure products:
  * halite (NaCl),
  * sylvite (KCl),
  * anhydrite ($CaSO_4$),
  * gypsum ($CaSO_4$, $2H_2O$),
  * kieserite ($MgSO_4$, H_2O), and
  * polyhalite ($K_2Ca_2Mg(SO_4)_4$, $2H_2O$);
  *carnallite ($MgCl_2KCl$, $6H_2O$) could not be procured in sufficient quantity; and

- samples of steel to observe the effect of the simultaneous action of radiation and salt on steel corrosion. These experiments are useful in relation to the construction of steel containers or overpacks for radioactive waste repositories in salt formations.

2.4. Method of Sample Packaging

Before being irradiated, the salt samples were packaged in a special vessel able to retain the gases produced for later analysis. This vial was designed to be gastight up to few bars and resistant to temperature, gamma rays and corrosion by salt or brine. Attenuation of gamma-rays should also be as low as possible.

The design of the irradiation vial was determined after preliminary tests involving crushed salt irradiated under an atmosphere of synthetic air.

The vial is designed to enclose 200 g of crushed salt and fit a certain geometry, with free volume equal to the apparent volume of the salt. A ratio of A/v = 1/3 was maintained throughout the program, except for the 50 mm diameter core drillings, where A/v is equal to 1/4, because otherwise the sample would heat up during vial sealing. A is the free volume left by the salt and v is the real volume of the salt, calculated from its mass and density.

The vial selected is manufactured from a tube of Pyrex glass measuring 44 mm in diameter and 330 mm long (Fig. 1). Its sealing concept prevents the introduction of water vapor or combustion gas during sealingwhich is done by welding the glass.
At one end he vial has a 12 mm and 6 mm diameter neck pipes, one for salt filling and the other for pumping and re-filling the selected atmosphere.

The other end of the vial is closed with a "pig tail" inside a 12 mm diameter neck pipe ; a 19/9 female connector is welded to this end after irradiation. A magnetic Teflon-coated bar (ϕ = 7 mm, L = 60 mm) is introduced for later break off of the pig tail. Then a glass/metal valve with grease-free connectors is added, so that the vial can be adjusted to fit different analytical apparatus and, samples of a given quantity of gas can be taken without any pollution.

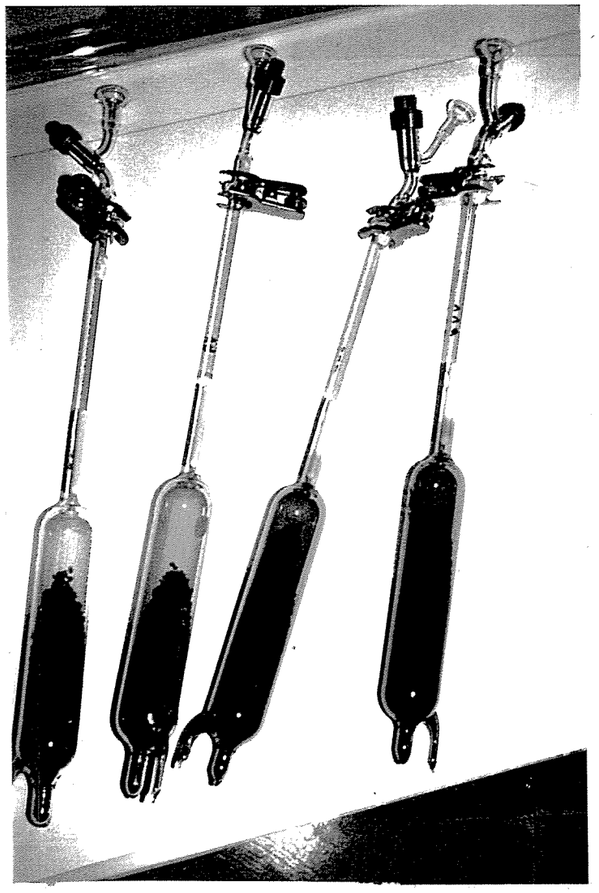

Figure 1: *Vials after irradiation, fitted for gas analysis*

Each vial has and engraved number and is heated to 500°C before use.

Most irradiations were performed on 200 g samples of crushed salt. Three irradiations were performed simultaneously on the same sample as well as on a blank of selected atmosphere to determine the order of magnitude of the deviation in the measurements. However, after a program delay incurred when the irradiator was off-line (November 1989 to July 1990), irradiations were first performed in groups of eight on two levels in the irradiator, then vial diameter was reduced to 40 mm while maintaining the A/v ratio; the irradiated salt mass was 150 g. The good test reproducibility and reliability of test methods also allowed the reduction in gas volume to be analyzed.

Fig 2 : *Coloration of salt samples irradiated at different doses*

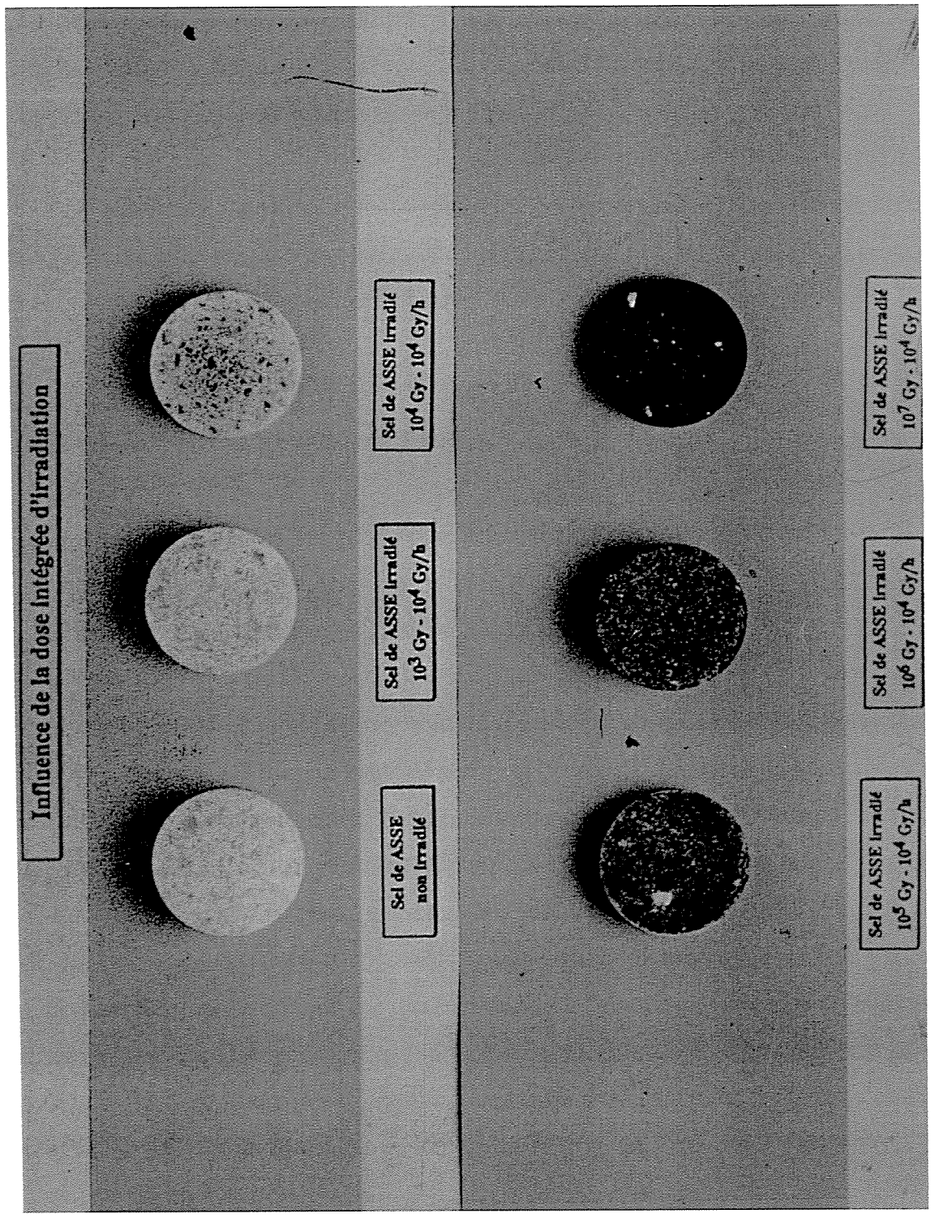

The samples must be prepared carefully to control initial conditions and ensure good test reproducibility. The set of four vials is filled with salt, then the air in the vials is expelled for one minute and replaced with an atmosphere of known composition at less than atmospheric pressure. This atmosphere could be N50 reconstituted air, inert gas, oxygen or media in a 50/50 or 20/80 N_2/O_2 ratio supplied by Air Liquide/Alphagaz. This operation is repeated three times before the vials are sealed. The final packaging pressure is 930 mb.

After irradiation, the vial receive the valves and connectors described above. A vacuum pumping of these parts removes any traces of humidity or pollution before releasing the gases by breaking the pig tail with the magnetic bar.

3. POST-IRRADIATION PROCEDURES.

This section describes the procedures selected to analyze the different products of irradiation namely: to study of radiation damage in the halite crystals of the salt rock, and to study the gases released by radiolysis of the salt rock.

Gamma rays induce radiolytic reactions in constituents of a saline medium, particularly water, fluid inclusions and the salt itself. When γ rays enter a solid, Compton electrons can be produced. As these electrons move, they produce ionization along their trajectory. In alkali halides, such as sodium chloride, excited Cl^- ions can be ejected from their normal position in the lattice leaving behind them an electron. The void left behind by the chlorine with the trapped electron constitute the F centers which agglomeration produces Na colloids regions in the crystal. The chlorine itself occupies an interstitial position giving rise to H-center development. The F centers are responsible for the brownish yellow coloration observed at low doses. The colloidal particles of metallic sodium are responsible for the blue coloration observed in the samples of salt irradiated at high doses (Fig. 2).

Different techniques, described below, to analyze gases were developed gradually as the experimental program advanced.

Basically, these techniques are, on one hand, mass spectrometry to analyze hydrogen and constituents of the atmosphere (N_2, O_2, possible traces of argon) and of NO, principally in the blanks of synthetic air, and, on the other hand, gas chromatography for systematically analyzed compounds such as CO_2, N_2O, CO and CH_4.

Based on results of the foregoing, different supplemental analyses to detect SO_2, H_2S, HCl, etc., that may be present after irradiations at a high total dose.

3.1. Method of Colloidal Sodium Content Determination .

Analysis of the amount of sodium colloid contained in the samples irradiated in this program took place by dissolving them in water and measuring the produced hydrogen. This indirect determination method is based on the assumption that every two Na atoms from the colloids will decompose two water molecules and produce an hydrogen molecule and sodium hydroxide.

Irradiated salt is dissolved in deionized water to quantify the formation of defects from irradiation. The following reaction occurs :

$$2\ Na^+e^- + 2\ H_2O \geq H_2 + 2\ Na^+ + 2\ OH^-$$

The hydrogen content measured by mass spectrometry enables observation of sodium colloid formation. Four grams of irradiated salt are poured in a flask which is then vacuum emptied. Then 20 ml of deionized water are introduced through a septum. Bubbles observed when water is added correspond to the formation of hydrogen. Dissolution lasts approximately one hour, then the flask is cooled with liquid nitrogen to trap the water before analysis by mass spectrometry.

3.2. Direct Mass Spectrometry Methodology

The spectrometer used to analyze light gases (atomic weight< 200) is an apparatus with single focusing magnetic sectors manufactured by the CEA. Separation is carried out by a magnetic prism producing an homogeneous field perpendicular to the ion beam. The resolution of this type of apparatus under normal conditions is 250. The pipe of introduction is made of stainless steel and completely tight (vacuum < 10^{-5} torrs). The mixture to be studied is released into a flask calibrated to a working pressure of approx. 1 torr, measured with a membrane micromanometer. The interface between the flask and the spectrometer source is a molecular leak of 30 lusecs (millitorr-liter per second). The fragmentation of each compound and the sensitivity of each gas must be known before proceeding to an examination of the spectrum (signal/pressure ratio of the source). Standard gaseous mixtures are used for calibration.

The results of mixture compositions are estimated in relation to nitrogen content, which is assumed to be constant. Gamma irradiations at total doses higher than 10^7 Gy have revealed variation in the N_2/O_2 ratios and the formation of nitrogen oxides. A future experiment might introduce a noble gas into the composition of the irradiation atmosphere, such as neon, which is very easily detectable by mass spectrometry and unaffected by radiolysis. Deeper studies of the absorption of nitrogenated compounds by salt could be perform by marking the air with ^{15}N. The hydrogen detection limit of 3 ppm in volume made it possible to observe this gas even after irradiations at very low integrated doses (10^3 Gy). NO content values did not give rise to any special calibration.

3.3. Gaseous Phase Chromatography (GPC) Methodology

Two types of chromatographic separation analysis with an identical "on-column" injection system were used. Because the quantities of the different compounds to be detected could be very low, we established a fixed gas injection volume of 2 ml (injection loop) when performing the first tests. The adaptation of a six-way valve, when used in different positions, allows the column to be flushed, the sampling system and sampling loop to be degassed, and the sampled fraction to be carried away for chromatographic separation with the carrier gas. Under

these conditions, the injected volume remains constant, both for the calibrating standard and for the sample. Sample or standard pressure at injection is measured with a manometer.

The mixtures of calibrating standards in nitrogen make it possible to obtain the respective calibration curves of the analyzed compounds by dilution in a known volume of nitrogen using volumetric flasks. In these calibration curves the peak area obtained at the characteristic retention time of the analyzed compound is plotted as a function of its concentration. The partial pressures are taken into account when interpreting the results.

The methods and conditions used to analyze the different compounds were :

- Chromatography with catharometric detection for analysis of CO_2 and N_2O: Separation is done on a steel column measuring 1/8" in diameter and 3 m long packed with a material made of 80-100 mesh porous polymer beads (Porapack Q, Chrompack); helium is the carrier gas (16 ml/min) and a constant temperature of 30°C is maintained during analysis. Catharometric detection is carried out with a 600 ml cell containing four WX (tungsten-rhenium) filaments fed with a 200 mA current and heated to 50°C. This equipment enables also measurement of CO (> 40 ppm in volume).

- Flame ionization detection after methanation : Because chromatographic separation on a molecular sieve followed by catharometric detection to analyze traces of CO is not sensitive enough, flame ionization detection is used. Hydrogen (15 ml/min) is the carrier gas for separation. The 2 m long, 1/8" diameter steel column is packed with a 60-80 mesh molecular screen and heated to 30°C. Hydrogen reduction of CO into CH_4 occurs in a platinum sponge furnace heated to 350°C.

- Chromatography with flame ionization detection for CH_4 and light hydrocarbons with a molecular weight of less than 60: Separation take place in a 3 m long, 1/8" diameter steel column packed with 50-80 mesh porous polymer (Porapack T, Chrompack), whose polarity is greater than that of Porapack Q, with helium as

the carrier gas. The flame ionization detector (q = 250°C) uses a hydrogen flame burning in air. Separation of the other hydrocarbons is achieved by increasing the temperature of the sample from 30 to 120°C with a rate of 10°C/min.

Flame photometry detection (FPD) of SO_2 and H_2S was planned after chromatographic separation at a temperature of 80°C in a 1/8" glass column packed with 80-100 mesh Tenax (preheated during 2 hours at 100°C), with the detector temperature raised to 140°C. Feasibility tests served to define detection limits of 5 ppm for H_2S and 0.2 ppm for SO_2 in the case of a calibrating mixture in nitrogen. The advantages of flame photometry are the simultaneous detection of sulfured compounds and the time saved over the combined chromatography/mass spectrometry technique. Detection can be improved by injecting a larger volume (2 ml) with a valve that is inert to sulfured products.

Gaseous chlorine detection by GPC with flame ionization detection: For simultaneous analysis of chlorine and hypochlorite contained in the gaseous phase, the property of phenols to react with these species by an electrophilic substitution mechanism is used. All or part of the available mixture in the vial is complexed with a 2.6 dimethylphenol (DMP) solution in a 0.05 M sulfuric medium. The chloro-4-DMP complex is extracted in an n-hexane medium and can be concentrated to improve sensitivity (this was done for low doses of radiation). The presence of an internal standard, such as chloro-4 dimethylphenol-3.5, makes it possible to observe the progress of the operations. After injection of the sample at a temperature of 230°C, chromatographic separation is done in helium. The column used is a CP-sil-5-CB semi-capillary column (Chrompack) of apolar melted silica measuring 25 m long with a 0.53 mm inner diameter and a phase thickness of 5 µm. Detection is done by flame ionization with a furnace temperature programmed from 80 to 200°C. Calibration curves based on a calibrating mixture of 1000 ppm of Cl_2 in nitrogen were plotted.

3.4. Gaseous Phase Chromatography Coupled with Mass Spectrometry Methodology

The coupling of a fragmentation technique such as chromatography with an analytical technique such as mass spectrometry makes it possible to achieve good detection sensitivities for compounds in trace amounts. Analysis may be qualitative or quantitative. In the first case, the spectrometer is used to scan the magnetic field to achieve a mass spectrum or currentogram; in the second case, it is used for fragmentography. In the second case, the apparatus is set, in succession, for each ion characteristic of the compound to be analyzed or that has the least amount of interference with another compound by varying the source's acceleration voltage with the computer control system.

This technique was used to identify SO_2 and H_2S after irradiation. In this case, the operating conditions were as follows:

- glass chromatographic column (1/4" dia. and 2 m long) filled with 80-100 mesh Tenax;
- two constant temperature chromatographic separations: 25°C for H_2S and 50°C for SO_2;
- a VG 7035 magnetic spectrometer with a resolution of 2000;
- quantitative analysis based on fragmentation by observing characteristic ions:

-	ions 64 and 66 for SO_2	$^{32}S\ ^{16}O\ ^{16}O$ and $^{34}S\ ^{16}O\ ^{16}O$
-	ions 34 and 33 for H_2S	$^{1}H^{1}H^{32}S$ and $^{1}H^{33}S$* for ion 34,
		$^{1}H^{32}S$ and ^{33}S* for ion 33
		(* being very low)

The product is identified in this manner by three criteria : its chromatographic retention time, the two characteristic ions and the concentration ratio of these two ions (for example, for SO_2, the 66/64 = 4% ratio corresponds to the natural isotopic ratio of $^{34}S/^{32}S$).

The quantitative range of analysis is 1 to 50 ppm. Calibrations are performed using standard mixtures in nitrogen supplied by Air Liquid/Alphagaz (500 ppm content), by dilution in vials with unlubricated spigots and with a LB1 "thermogreen" septum (Supelco). These dilutions are not stable for more than one week.

Chromatographic separation for analysis of SO_2 made identification of Cl_2 possible. The chlorine present in the currentogram upstream from the SO_2 disturbs measurement of the latter, mainly at high doses. Direct quantitative analysis of gaseous chlorine is not feasible with this technique, since this element is rapidly trapped on the metal sections of the apparatus.

3.5. Ion Chromatography Methodology

From the irradiated vial, two samples of gas are simultaneously taken into two 20 ml calibrated flasks. Then, all of the chloride ions as well as the other anionic species are trapped in 5 ml of an NaOH 10^{-4}M solution. To obtain all of the chloride ions, the transformation of the ClO^- ions into Cl^- is accelerated by the addition of 100 ml of H_2O_2. Analysis is done after separation in an HR anionic column (Waters) by conductimetric detection and determination of the areas of characteristic peaks. Calibration based on sampling of gaseous compounds in the nitrogen is done under identical conditions. By proceeding in this manner, the "total chlorides" concentration of the gaseous mixture analyzed is derived; the concentration of hydrochloric gas is the difference:

[total chloride] - [chloride + hypochlorite]

3.6. Fourier Transform InfraRed Spectrometry Methodology

Analysis by infrared spectrometry of the asymmetric gaseous compounds is based on the excitation of different types of molecular movements : rotation and vibration. The energies corresponding to these movements lead to absorptions of electromagnetic radiation characteristic of the molecules observed. The rotational absorption spectra are located in the outer infrared band (0.1 to 200 cm^{-1}). The vibrational absorption spectra, often associated with vibration-rotation movements, in the case of gases, is located in the spectral range of medium infrared (200 to 4000 cm^{-1}), This was therefore the analytical range chosen to perform analysis of the gaseous compounds developed or liberated during our irradiation experiments (CO_2, N_2O, CO, NO, NO_2, HCl, CH_4, hydrocarbons,H_2O).

The improvements introduced by us on the existing standard method consisted of adaptation of the sampling and measuring cell, and modification of data processing in order to allow quantitative analysis to take place. It was necessary to constitute a library of standards of each compound studied as a function of temperature.

The apparatus used is an IFS 48 from Bruker equipped with a mercury, cadmium, tellurium (MCT) detector cooled with liquid nitrogen for use in the medium infrared (600-4000 cm^{-1}) range. IR radiation is emitted by a source of silicon carbide cooled by water. In order to study the detailed structure of the gas molecules, we work with a resolution of 0.5 cm^{-1}.

The IR beam crosses the measuring cell, where the gaseous sample is enclosed, before being detected. A special cell for the analysis of corrosive gases (Fig. 3) has been developed in the framework of this program in cooperation with the Bruker/Spectrospin company. This cell is small (100 ml), but the length of the optical path is increased by using mirrors. This path is adjustable from 25 cm to 1 meter by acting upon the concavity of one of the reflex mirrors with a micrometric screw. The number of reflections thus ranges from 4 to 16. The choice of materials is important; Pyrex was chosen for the body of the cell, and the windows are in BaF_2. This material offers the advantage of being less soluble than KBr and more resistant to light and temperature than standard materials (such as AgBr). The cut-off of the spectrum is around 800 cm^{-1}. The mirrors of the cell are gold-plated and their supports are of Teflon. The cell can be heated to 200°C.

The analysis is made more complex by the presence of molecules whose spectrum characteristic rays can superpose. Because the range of concentrations of certain major compounds such as CO_2 and N_2O can vary from a few ppm to several % in volume, the choice of specific rays that are unsaturated and without overlap is restricted for the analysis of the other constituents. However, quantitative analysis was possible by combining a certain number of standards which spectrum rays are on either side of the sample spectrum, with a sufficient number of characteristic rays, up to ten.

The processing software (GAZ) [GAUDEZ & al 1993] developed over the course of this study is based on the principle of multipeak analysis. It permits determination of the

content of each of the compounds in the mixture, and takes into account the possible non-linearity of detection.

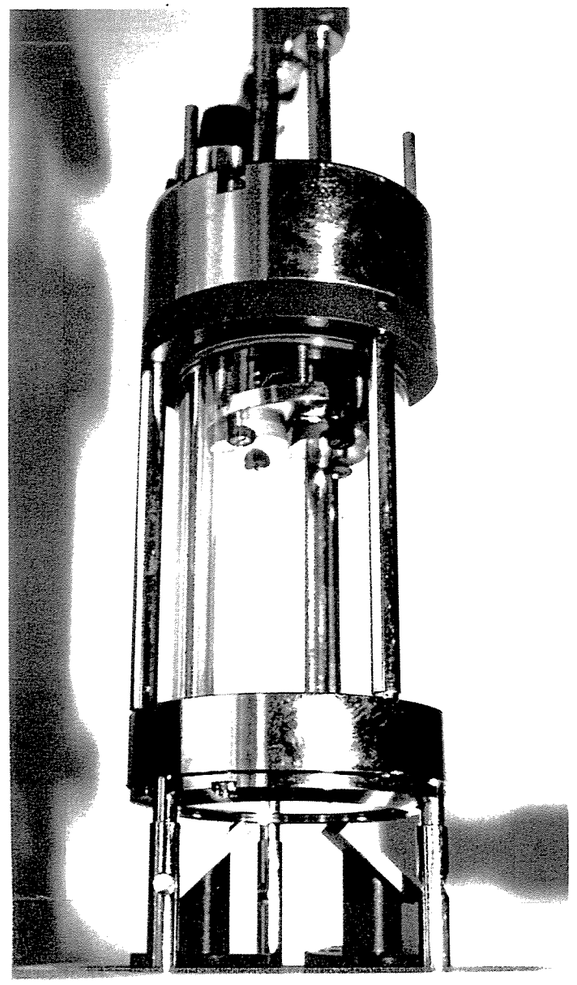

Figure 3 : *Cell developed for FITR spectroscopy*

3.7. Detection Limits for Different Gases

The adaptations to the apparatus and the analytical procedures described previously allowed to reach the detection limits listed in Tables 3 and 4 and expressed in ppm (mg of gas formed by kg of salt (mg/kg_{salt})).

Table 3 : *Detection Limits (mg/kg_{salt}) of Mass Spectrometry and Chromatography*

CO_2	N_2O	CO	CH_4	H_2	SO_2	H_2S	Cl^-	Cl_2
10^{-2}	10^{-2}	$5 . 10^{-4}$	10^{-4}	$3 . 10^{-4}$	$5 . 10^{-2}$	10^{-2}	10^{-1}	$2 . 10^{-1}$

Table 4 : *Detection Limits (mg/kg_{salt}) of FTIR/Gas at Ambient Temperature*

CO_2	N_2O	NO	CO	NO_2	HNO_2	HNO_3	CH_4	C_2H_6	C_2H_4	HCl	SO_2
10^{-2}	10^{-2}	10^{-2}	10^{-2}	5.10^{-3}	5.10^{-3}	2.10^{-2}	5.10^{-3}	10^{-2}	10^{-2}	10^{-2}	5.10^{-2}

4. RESULTS OF PRE-IRRADIATION DETERMINATION

4.1. Mineralogical and Chemical Composition

The granulometry of the salt delivered in August 1988 is very heterogeneous. Grain sizes vary from a few millimeters to the size of very fine dust. Moreover, salt blocks were observed, leading one to assume substantial humidity. The mineralogical compositions of the batches supplied by our colleagues of GSF/IfT and their water contents are given in Tables 5 and 6.

Table 5: *Mineralogical composition of Asse Salt (Batch I)*

Mineral Phase	Halite	Polyhalite	Anhydrite	Others	H_2O
Mass % (mineralogical analysis)	95.2	0.8	3.8	< 0.3	0.066

Table 6 : *Mineralogical composition of Asse Salt (August 1988)*

Mineral Phase	Halite	Polyhalite	Anhydrite	Kieserite	H_2O	Carbonates
Mass % (mineralogical analysis)	91.39	3.53	5.08			
Mass % (chemical analysis)	92.84	3.82	3.06	0.06	0.24	0.10

CEA performed additional chemical analyses on the final batch with the following results:

- CO_3^{2-} analyzed with exclusion chromatography — < 0.1% mass
- SO_4^{2-} analyzed by ion chromatography — [1.98 ± 0.02] % mass
- Cl^- analyzed by potentiometry — [58.0 ± 0.5] % mass

Total organic carbon (TOC) of this batch is [8 ± 3] ppm

Cation distribution is given in Table 7.

Table 7 : *Cation composition*

Mineral	Na	K	Ca	Mg	Al	Si	Fe
mg / gram of salt	230	10	0.95	0.23	0.064	<0.005	<0.005

4.2. Composition of Fluid Inclusions.

The charged particle spectra obtained with the Nuclear Microprobe?? make it possible to identify three types of fluid inclusions : fluid inclusions with hydrocarbons, with brine and fluid inclusions with both hydrocarbons and brine (Fig. 4).

Inclusions' carbon and oxygen content have been calculated for each spectrum by subtracting the contribution of the salt, deduced from α particle signals characteristic of chlorine that are emitted at a higher energy than the carbon protons. Corrections in the measurements were made to take into account interferences existing on the carbon and oxygen proton signals. These interferences were attributed to charged particles (alphas) produced by sodium and chlorine. They were estimated from an halite piece devoid of fluid inclusions.

Secondly, and despite rather poor counting statistics, oxygen contents were estimated from the p_o signal (see Fig. 4) because of intense interferences with salt signals in the p_1 proton regions. From the non-offset position, in relation to information from the surface, of the carbon

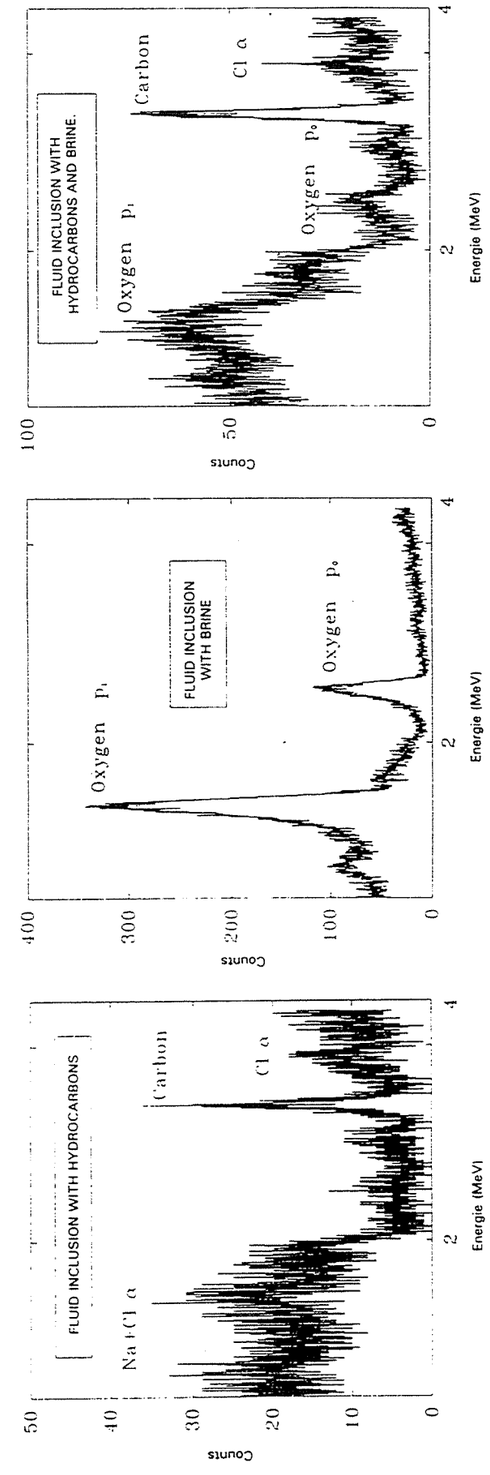

Figure 4 : *Fluid inclusions analyzed with nuclear microprobe*

and oxygen peaks and their width at mid-height, the following information can be deduced:

- in the biphased inclusion, an approximately 2 μm thick, low-density, carbon-rich layer covers the surface of the inclusion ; it could be liquid methane;

- inclusions with hydrocarbons and biphased inclusions with hydrocarbons and brine are small in size: 30 μm wide and a maximum of approximately 5 μm thick; the brine inclusion is 5 μm wide and 7 μm thick.

Measured carbon and oxygen contents are, respectively, 0.015 mol cm^{-3} of carbon in the inclusion with hydrocarbons, 0.01 mol cm^{-3} of oxygen in the biphased inclusion and 0.08 mol cm^{-3} of oxygen in the inclusion with brine only. For the latter inclusion, the measured oxygen content based on the gamma photon signal is 0.04 mol cm^{-3}. Analytical accuracy is 50% due to corrections for salt and germanium contributions. Measured carbon and oxygen contents for pure constituents correspond to the contents in pure water and methane.

The overlap of the different techniques enabled us to specify the composition of the fluid inclusions, esp. presence of carbon and heterogeneity of chemical composition from one fluid inclusion to another in the same sample; the inclusions may be rich in carbon and/or oxygen.

5. RESULTS OF POST-IRRADIATION ANALYSIS

The results from nearly 350 experiments were provided as work progressed and in the framework of meetings of the CEC/B1 (Asse) project committee. Most of the irradiations planned at 10^{-3} Gy/hr for 0.1, 1 and 10 hours were not carried out because the quantities of the gaseous compounds, CO_2 and N_2O, which were expected to develop, laid at the level of the detection limits.

5.1. The Determined Amount of Colloids.

Samples irradiated in a synthetic air atmosphere with a dose rate of 10^4 Gy/hr at 50°C, were dissolved in H_2O and the amount of hydrogen obtained was measured. The Hydrogen results show that the amount of Na colloids developed by irradiation increases as a function of the integrated dose. The photograph in Fig. 2 shows the blue coloration of the salt caused by the development of colloidal sodium particles. The amount of hydrogen which can be obtained by dissolving the samples containing colloids can be expressed as :

$$\text{hydrogen} = K\ (\text{Integrated Dose})^{x}$$

with x = 0.64 fromthe plot of Fig. 5b in the irradiation conditions (dose rate and temperature).

The amount of colloids developed in samples irradiated at temperatures of 50 to 250°C, with a dose rate of 10^4 Gy·hr^{-1} and an integrated dose of 10^6 Gy reaches a maximum between 100 to 150°C. It is linked to the mobility of the F centers and to the facility of diffusion of sodium atoms based on colloidal particles of metallic sodium, both of which depend on temperature.

The results obtained for samples of salt with different grain sizes, irradiated with a dose rate of 10^4 Gy/hr and an integrated dose of 10^6 Gy at 50°C in a synthetic air medium shows that the formation of colloids is greater when the salt is crushed more finely.

The production of sodium colloids increases slightly when the dose rate increases between 10^3 and 10^5 Gy/hr.

5.2. Results of Analysis of Gases Released During Radiolysis

The gaseous compounds present in the vial after irradiation can be formed or released either from the atmosphere surrounding the salt (whether oxidizing, reducing or inert) or from the salt sample itself including crystalline matrix (mainly halite), secondary minerals, adsorbed gases and fluid inclusions.

Figures 5 and 6 as well as the attached result curves (Fig. 7 to 26) make it possible to observe the different interpretations presented hereunder.

In the Fig. 7 to 26, the contents of the different gaseous compounds are expressed in μmole per kilogram of salt in order to better point up the importance of hydrogen in the mechanisms in play.

5.2.1. Evolution of the Filling Atmosphere.

For irradiations done in synthetic air atmosphere, the O_2/N_2 ratio, initially at 0.25, is monitored as a function of the total dose. For an integrated dose of 10^6 Gy, variations of the dose rate from 10^2 and 10^5 Gy·hr^{-1} does not affect this ratio.

This ratio, which is practically constant as a function of the integrated dose up to 10^6 Gy, decreases rapidly beyond 10^7 Gy. This is explained by the consumption of the oxygen of the filling atmosphere related to the formation of CO_2. High temperatures enhance this phenomenon.

The drop of the O_2/N_2 ratio above total doses of 10^7 Gy has been observed for two different granulometries as plotted in Fig. 10 and 11($.1<\phi<.25$ mm and $1<\phi<2$ mm).

Irradiations of batches of salt of different granulometries did not reveal a variation in the O_2/N_2 ratio. However, during irradiation at 10^4 Gy/hr for a dose of 10^6 Gy, for the batch of salt whose particle diameter is from 0.125 to 0.25 mm, the formation of CO_2 is abnormally high. The explanation proposed by our German colleagues was a possible pollution of the batch during its storage after crushing in the mining equipment.

Irradiations performed at 10^{+6} Gy in the presence of mixtures of oxygen and nitrogen with O_2/N_2 ratios of 50/50 or 20/80 (Fig. 17 and 18) hardly change the original ratios. However, a 10% decrease in the nitrogen content of one vial, initially filled with an O_2/N_2 ratio of 20/80 have been observed.

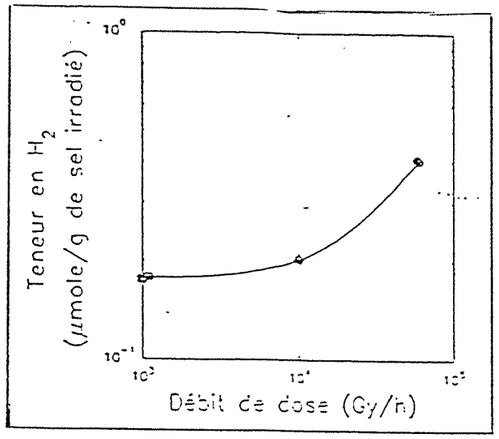

Figure 5a Production of colloidal sodium vs dose rate (10^6 Gy in air @ 50°c)

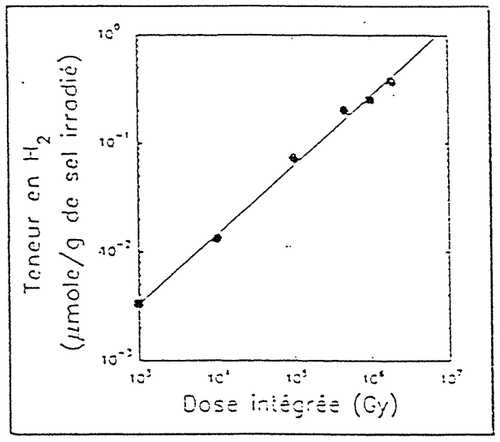

Figure 5b Production of defects in crystals vs integrated dose (10^4 Gy/h in air @ 50°c)

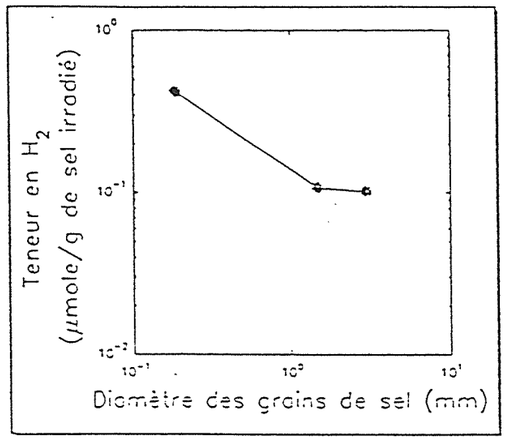

Figure 6a Formation of colloidal sodium vs grain size (10^4 Gy/h and 10^6 Gy in air @ 50°c)

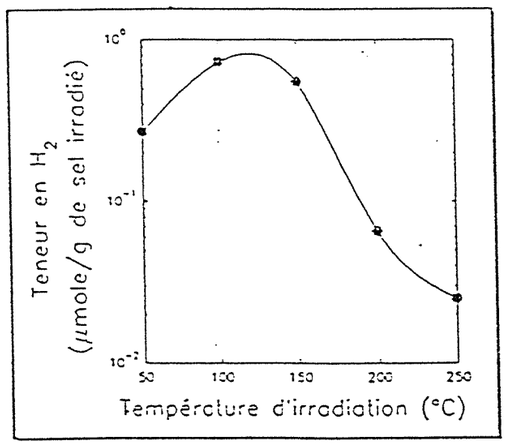

Figure 6b Formation of colloidal sodium vs temperature (10^4 Gy/h and 10^6 Gy in air)

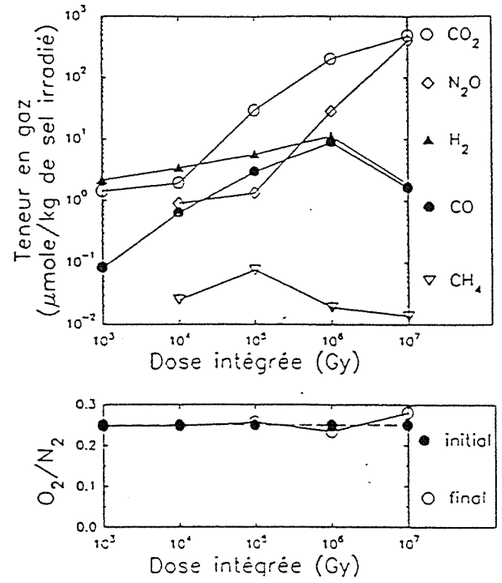

Figure 7 Gas production vs integrated dose (10^4 Gy/h in air @ 50°c)

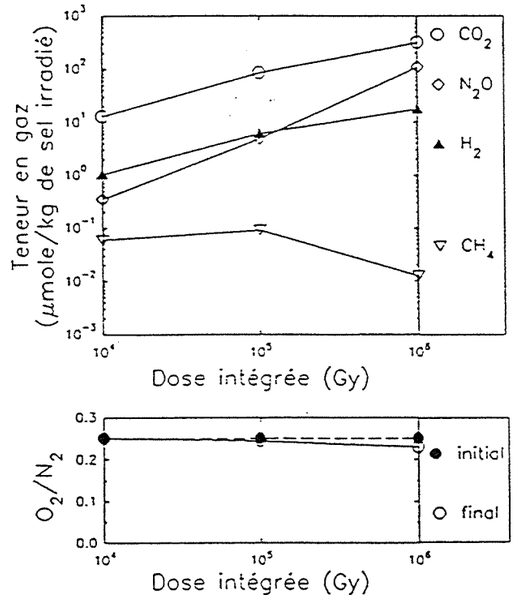

Figure 8 Gas production vs integrated dose (10^4 Gy/h in air @ 150°c)

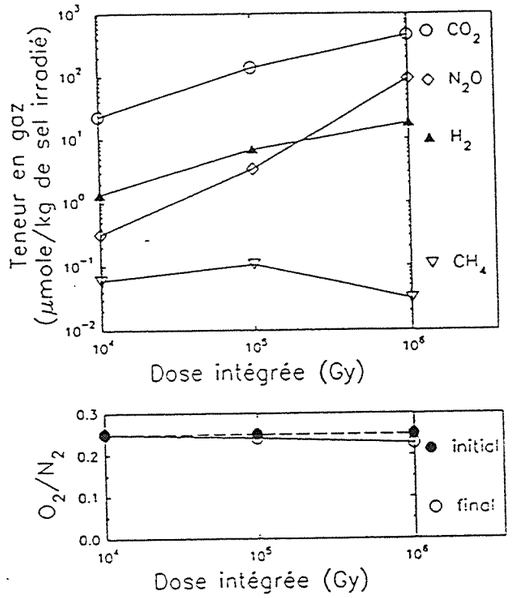

Figure 9 Gas production vs integrated dose (10^4 Gy/h in air @ 200°c)

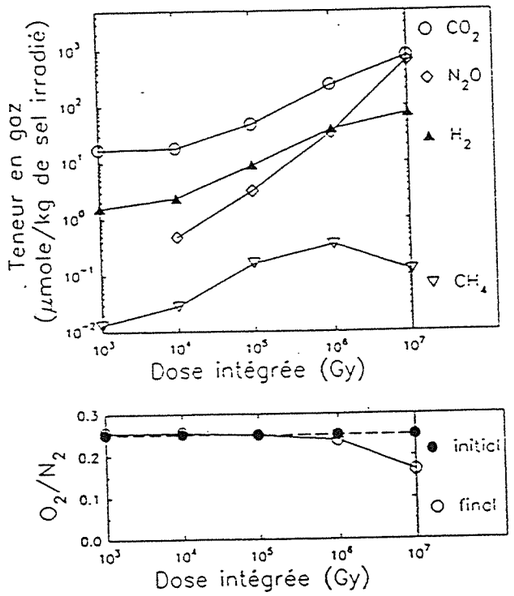

Figure 10 Gas production vs integrated dose : Grain size between 0.1 mm and 0.25 mm
(10^4 Gy/h in air @ 50°c)

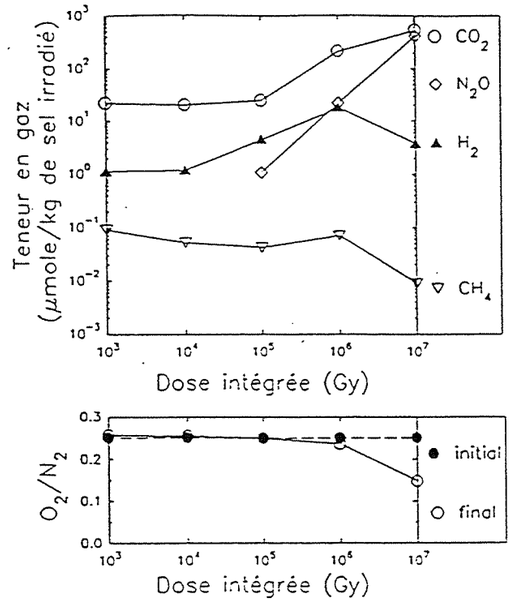

Figure 11 Gas production vs integrated dose : Grain size between 1 mm and 2 mm
(10^4 Gy/h in air @ 50°c)

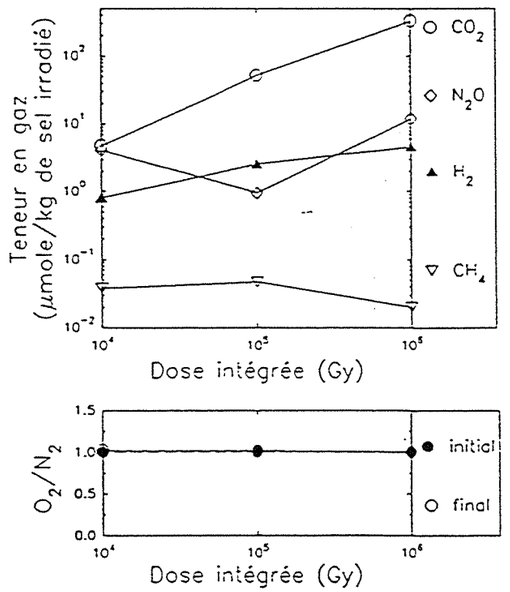

Figure 12 Gas production vs integrated dose : Initial filling gas 50% N_2 + 50% O_2
(10^4 Gy/h @ 50°c)

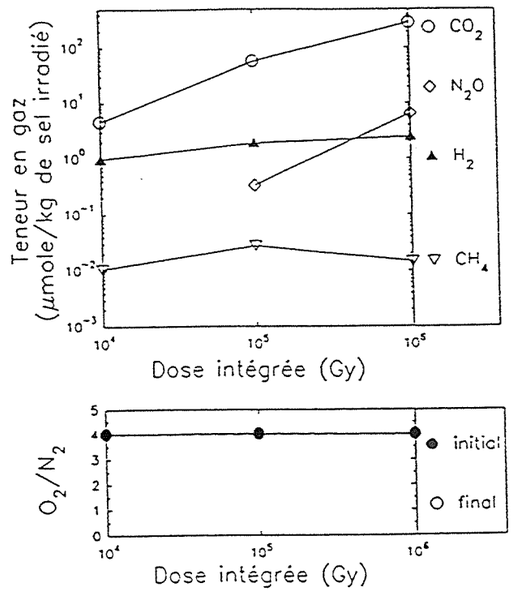

Figure 13 Gas production vs integrated dose : Initial filling gas 20% N_2 + 80% O_2 (10^4 Gy/h @ 50°c)

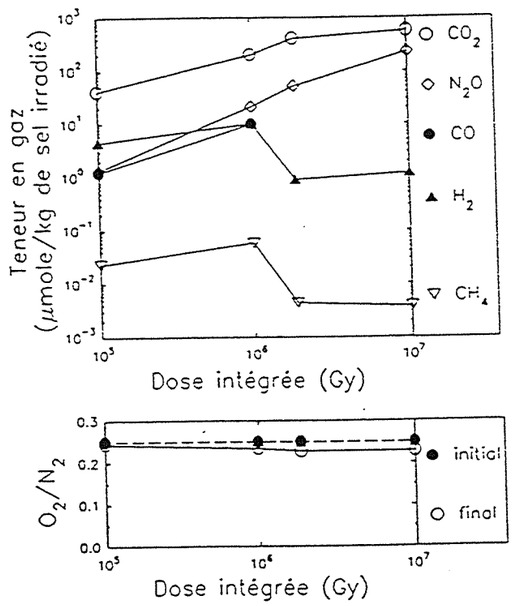

Figure 14 Gas production vs integrated dose (10^3 Gy/h in air @ 50°c)

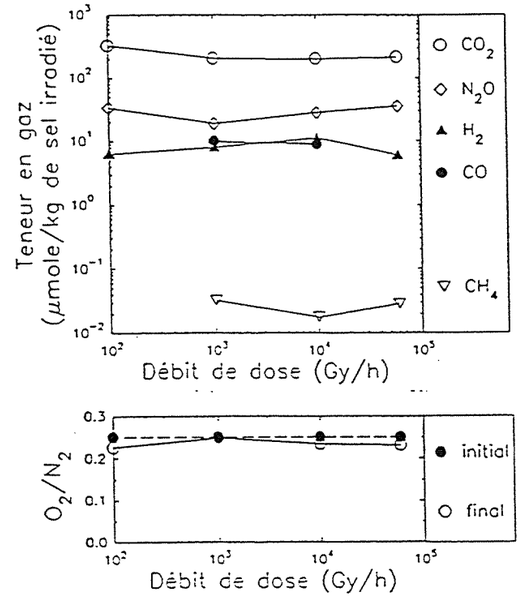

Figure 15 Gas production vs dose rate (10^6 Gy in air @ 50°c)

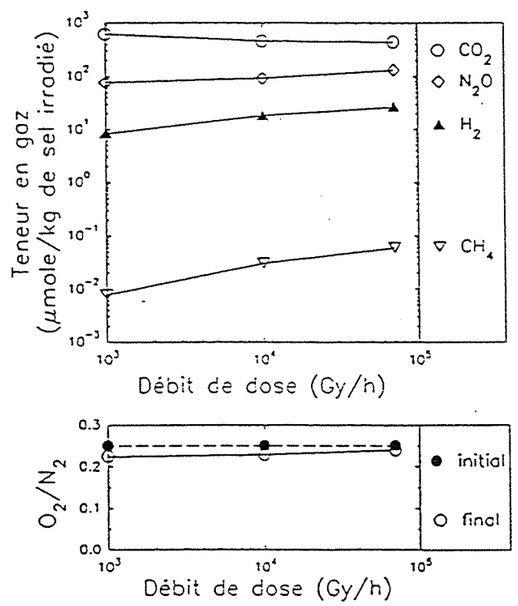

Figure 16 Gas production vs dose rate (10^6 Gy in air @ 200°c)

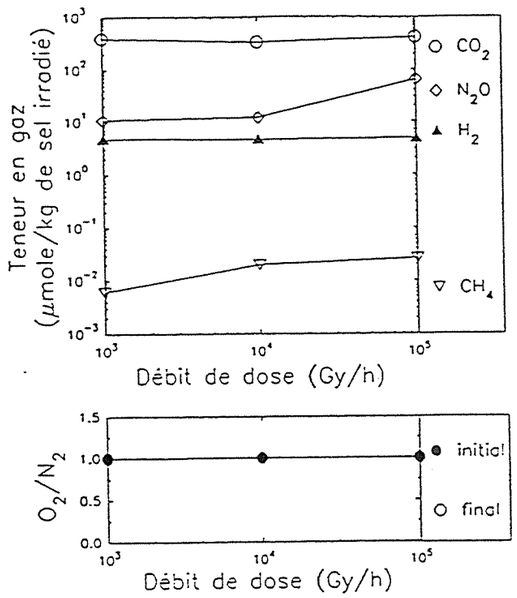

Figure 17 Gas production vs dose rate : Initial filling gas 50% O_2 + 50% N_2 (10^6 Gy @ 50°c)

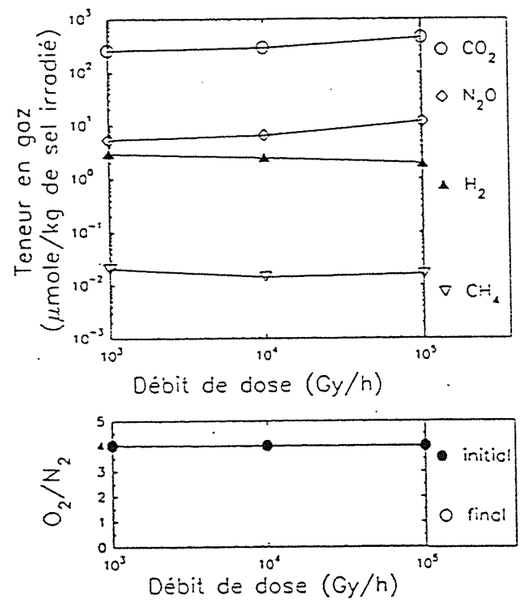

Figure 18 Gas production vs dose rate : Initial filling gas 20% N_2 + 80% O_2 (10^6 Gy @ 50°c)

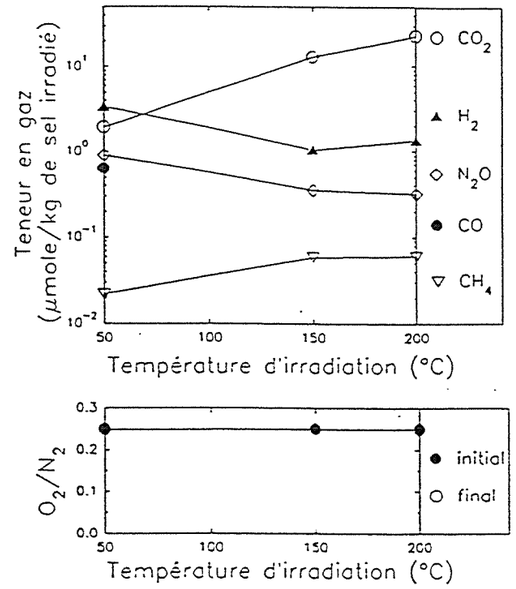

Figure 19 Gas production vs temperature (10^4 Gy/h - 10^4 Gy in air)

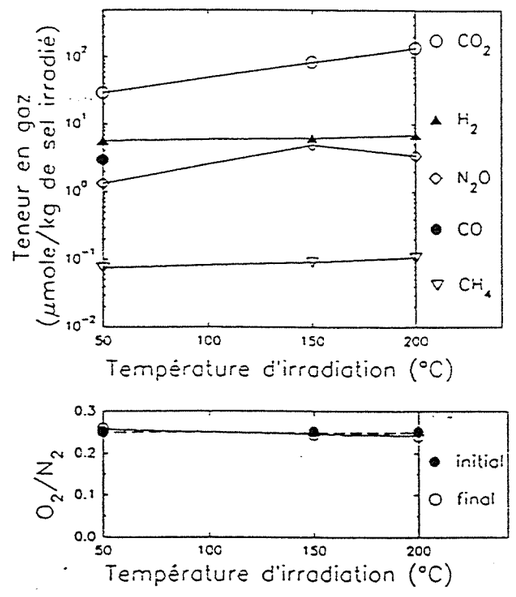

Figure 20 Gas production vs temperature (10^4 Gy/h - 10^5 Gy in air)

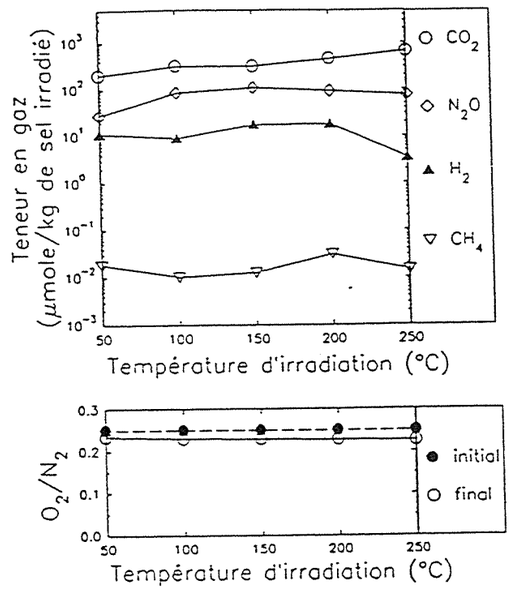

Figure 21 Gas production vs temperature (10^4 Gy/h - 10^6 Gy in air)

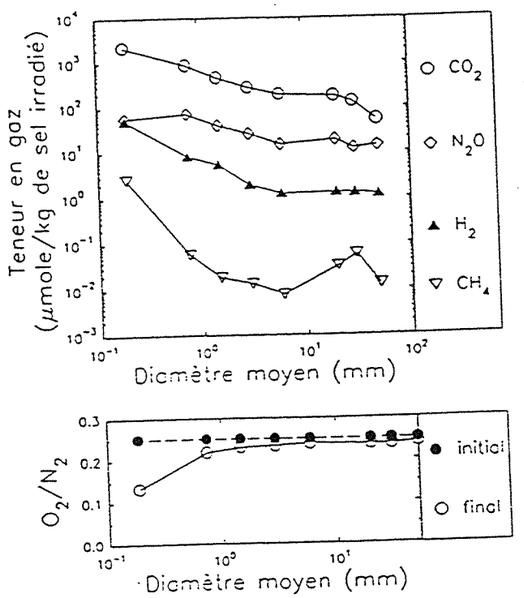

Figure 22 Gas production vs grainsize : Crushed salt and core samples
(10^4 Gy/h in air @ 50°C)

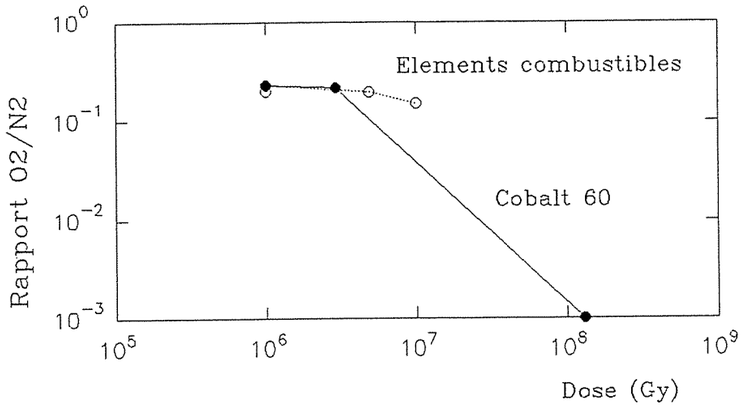

Figure 23 Evolution of O_2/N_2 ratio vs dose

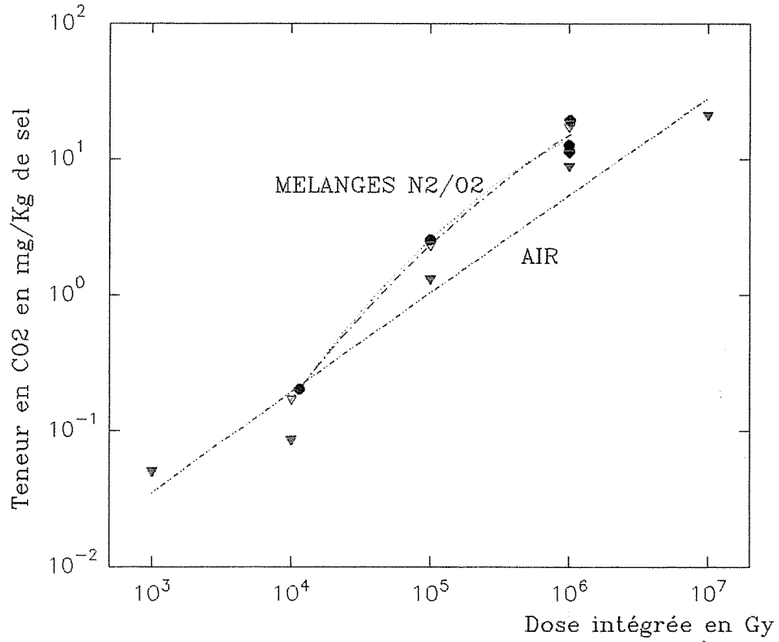

Figure 24 Evolution of CO_2 content vs O_2/N_2 ratio in the initial filling gas

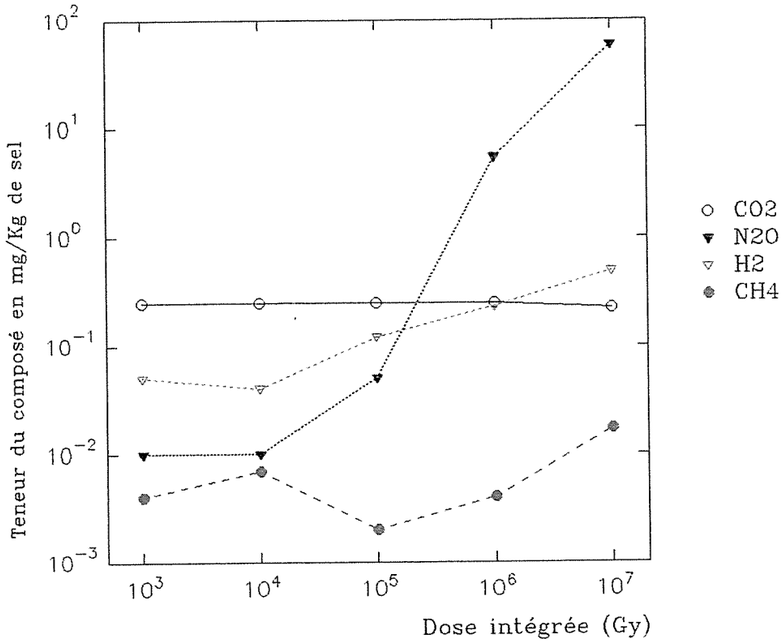

Figure 25 Evolution of irradiated blanks vs dose (10^4 Gy/h)
Blank = ampoule filled with air

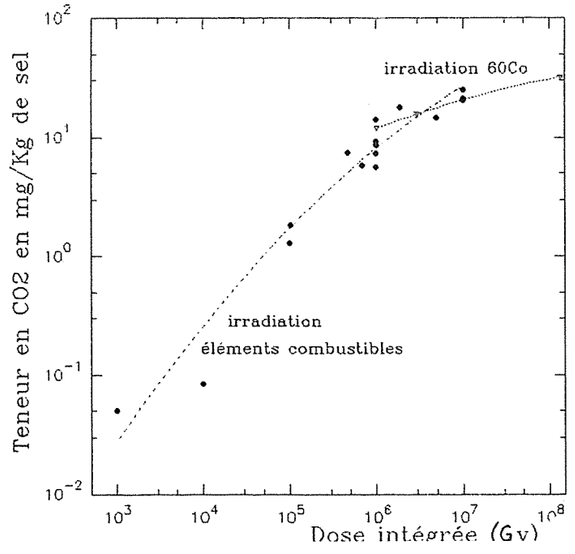

Figure 26 Evolution of CO_2 vs dose including irradiations with ^{60}Co

5.2.2. Type of Compounds Formed as a Function of the Filling Athmosphere.

The principal gaseous compounds released during γ irradiation observed as a function of the various parameters are: H_2, CO_2, N_2O, CH_4 and the initially present gas compounds. Others, such as CO, Cl_2, Cl^-, NO, SO_2, H_2S and the light hydrocarbons were identified during certain irradiations, mainly at high doses (> 10^7 Gy).

It is convenient for further study to distinguish between gases developed in an oxidizing atmosphere and those developed in an inert atmosphere. These two types of environments and of course the mixtures of O_2 and N_2 in a 50/50 and 20/80 ratio were studied during this program. An irradiation in vacuum with a dose rate of 10^4 Gy/hr and a dose of 10^6 Gy rounded off the study.

The composition of the gaseous phase in the repository will evolve over the course of time, with consumption of ambient oxygen; it would be interesting to pursue this study with mixtures whose O_2/N_2 ratio diminishes to observe the kinetics of formation of the different compounds indicated.

Compounds formed in an oxidizing medium: these are mainly N_2O and CO_2, which are the ultimate phases of the reactions. NO and CO were analyzed, these are no doubt intermediate compounds, principally detected during incomplete oxidation reactions.

Compounds formed in an inert medium or in vacuum: these are mainly H_2 and hydrocarbons.

6. INTERPRETATION

6.1. The origin of N_2O.

N_2O is due to radiolysis of the air, the quantities detected in the inert medium are close to the detection limits.

The sequence of reactions that bring the nitrogen oxides into play culminates, when the quantity of oxygen is sufficient, in the formation of N_2O. In the irradiation blanks, the presence of NO is explained by the oxidation reaction of $N_2 + O_2 - > 2$ NO. In the samples, the combination of N_2 with O_2 as $1/2\ O_2 + N_2 \rightarrow N_2O$ may be enhanced by the presence of salt.

The N_2O contents obtained during the desorption tests at 300°C of samples irradiated in synthetic air, when subject to heating for more than one day, are not higher than those obtained immediately after irradiation, confirming that this compound is an end product of the reaction.

The generation of N_2O decreases slightly as the samples grain size increases, as plotted Fig. 22. For equal volume and composition of the atmosphere, the gas included in the crushed salt is more affected by radiation when the grain size is smaller.

The quantities of N_2O increase with integrated dose as plotted Fig. 7. This has been confirmed by the comparison of the results obtained with real samples and those obtained with those of "air blanks" simultaneously irradiated under the same conditions (Fig. 25). In the whole experiment, the observation of N_2O in the blanks was a way to control that the irradiation was correct.

The dose rate (10^2 to 10^5 Gy/hr) does not influence the development of N_2O as it is plotted Fig. 15 for a constant total dose of 10^6 Gy.

The heated irradiations show that the production of N_2O seems to reach a maximum between 150 and 200°C for total doses of 10^5 and 10^6 Gy (Fig. 20 and 21). However, this was not confirmed at 10^4 Gy.

After irradiations carried out in an inert atmosphere, the N_2O contents are below the detection limit. The formation of N_2O depends on the presence of oxygen, as inferred from the results of an irradiation in synthetic air and reaching a total dose of 1.3 10^8 Gy (^{60}Co source), where the formation of other oxygenated compounds was related to reduction of N_2O yields.

The presence of HNO_2 (sometimes detected by FTIR) in the samples of irradiated air is

the result of a reaction of NO with water vapor.

It is not know whether salt has any influence on the radiolysis of air . Our results indicate the amount of air radilysis on the presence of salt, which is relevant for a repository.

6.2. The Origin of CO_2.

The CO_2 of the salt samples can be present as adsorbed or as gas in fluid inclusions which can be mono or polyphasic. Polyphasic fluid inclusions use to contain as well hydrocarbons.

Analyses by ESCA and FTIR showed that the carbon present in the salt is organic in origin. The content of total organic carbon (TOC) is 8 ppm.

A thermal desorption of a non-irradiated sample of crushed salt (batch 1988) packaged in synthetic air has been carried out up to 300°C for 24 hours. The analysis of the CO_2 produced give a value of 35 mg of CO_2 per kg of salt.

The generation of CO_2 takes place essentially in an oxidizing medium, the quantities formed in an inert medium are close to the detection limits.

The carbon dioxide development increases with total dose up to 10^6 Gy, then seems to reach a plateau at high doses (Fig. 7).

The dose rate has little influence on the release of CO_2 (Fig. 15 to 18).

The irradiations carried out to study the dependence of gas production on the temperature took place at various dose rates (10^3, 10^4 and 10^5 Gy/hr) and total doses (10^4, 10^5 and 10^6 Gy). The yields of CO_2 obtained from them show that at low doses, CO_2 development is enhanced by temperature (Fig. 15 and 16, and 19 to 21). For an irradiation at a total dose of 10^4 Gy, an increase of temperature 150°C increases the CO_2 yields in a factor of 10 ; at 10^5 Gy the same temperature rise encrease the CO_2 yields in a factor of 5. After irradiation at a

total dose of 10^6 Gy, heat seems having nearly no influence on CO_2 production.

At low dose rates, the CO_2 generation is intensified by the quicker decomposition of hydrocarbons.

The influence of the salt grain size, as well as salt core drillings diameter, on the compounds produced has been studied at a dose of 10^6 Gy and at ambient temperature (see Fig. 22). The results confirm that CO_2 generation increases as the granulometry decreases. The greater the specific surface area of the material, the easier the interaction of γ radiation will be with the organic compounds contained in the fluid inclusions.

At a high doses the oxidation reactions slow down because the oxygen originally present in the vial has been consumed already. This is inferred from an irradiation performed up to 1.3 10^8 Gy (using Co^{60} sources) and at 65°C (Fig. 26). The quantity obtained stabilized around 20 mg of CO_2 per kg of salt above 10^7 Gy.

The formation of carbon dioxide is closely related to that of the other compounds, such as CO, CH_4 and the existing hydrocarbons.

6.3. The Origin of H_2, CO, CH_4

In the studied gaseous phase, H_2, CO and CH_4 are less abundant than the rest of the gases. However, they provide valuable information on the reaction and on the equilibrium of the gaseous phase.

The *hydrogen* originates primarily by the action of gamma rays on the H_2O molecules and on the organic compounds present in the fluid inclusions.

Hydrogen yields reaches a maximum around 10^6 Gy then decreases at higher doses (10^7 Gy), for irradiations in synthetic air. However, a greatest content has been observed at 1.3 10^8 Gy. This may indicates that the reactions in play are interrupted by lack of O_2 and

formation of oxygenated radical-like compounds allowing linkages with H_2.

In an inert atmosphere, or in vacuum, where hydrogen cannot react with the oxygenated radicals which are also being developed by radiolysis, the yields of H_2 are higher than in other environments where these reactions are possible.

Some irradiations have been carried out with samples of steel introduced in the vials together with the salt. One of the products of steel corrosion is hydrogen, which develops due to the reaction of the brines contained in salt with the metal. Contrary to the expectations, the amount of H_2 produced within these steel containing vials is not significantly higher than that of other vials. Probably integrated doses of 10^6 Gy, with dose rate of 10^3 Gy/hr, and at temperatures of 200°C are not damaging enough to change the H_2 production.

The carbon monoxide production is a function of the integrated dose. In the presence of oxygen the amount of CO produced reaches a maximum at 10^6 Gy, and then decreases (Fig. 7). It is therefore inferred that CO is produced as a the results of the oxidation of the organic matter contained in the salt samples, but that provided the amount of oxygen is sufficient, CO_2 is produced to the expense of CO.

Hydrocarbons detected in our experiments have their origin in the organic mater contained in the salt samples. They use to be either absorbed at the surface of the grain or ocluded in the fluid inclussions. The organic mater undergoes radiolytic fragmentation during gamma irradiation. Heavy molecules can become light hydrocarbons in an iner environment. The hydrogen being produced by the brine hydrolysis can help in this fragmentation, and moreover there is an additional thermal fragmentation of heavy hydrocarbons which has to be taken into account. As a result of these processes in an inert environment mainly light hydrocarbons are found. The main product is methane, although C_2H_4, C_2H_6, C_2H_2 and C_3H_8 are also found in trace amounts. The amounts of ligth hydrocarbons other than methane are close to the detection limits of our methods.

In oxidizing environments, with increasing time, and dose, CH_4 becomes CO and finally CO_2 . Production of CH_4 at a dose rate of 10^4 Gy/h and at 50°C in a synthetic air

environment has been observed to reach a maximum at 10^5 Gy, and then decrease in coincidence with the start up of the oxidation of the organic material. However, for irradiations up to very high doses (130 MGy) CH_4 content can increase if the amount of exygen in the environment is depleted: CH_4 would be constantly produced by fragmentation but not be able to oxidize and become CO_2.

The characterization of the organic matter present in the salt inclusions would allow prediction of the formation of compounds from degradation during the radiolysis reactions.

7. CONCLUSIONS

The methodology developped and refined in the course of this research was adequated to produce the sought answers and can now be used to study the gas by radiolysis in other possible candidate host rocks for radioactive wast. It is important to remark that the detection limits were so low that they allow us to draw the following conclusions.

Two big groups of gas types can be distinguished amongst those generated during irradiation of salt; those gases obtained by radiaolysis of brine and salt, and those which are obtained by fragmentation and eventual oxidation of organic mater. We have found that small grain sizes enhance both types of gas generation.

The gases produced by radiolytic decomposition of brine and /or of the salt itself are mainly H_2 and Cl_2, and minor amounts of other chlorinated compounds. Their production mainly depends on total dose, temperature and dose rate. Besides this direct production of H_2, hydrogen could be produced in repositories in the eventuality of their accidental flooding. The water would then react with the sodium colloids produced in the rocks salt by radiation damage, and produce hydrogen, amongst other substances. The amounts of hydrogen produced would be proportional to that of sodium metal colloids.

The gases produced from, first fragmentation, and then eventual oxidation of originally heavy molecules of hydrocarbons, are mainly methane and carbon dioxide. Methane can

survive in higher or lower amounts depending on the oxidizing characteristics of the environment. In oxydating environments it will oxidize up to carbon dioxide, but if the environment is depleted in oxygen, the production of methane would be enhanced, at least relatively to that of carbon dioxide. Intermediate products can as well develop, e.g. carbon monoxide.

The amount of produced gases is limited by the volume of rocksalt affected by the radiation and the temperature encrease on one hand, and on the other hand by the amount of source material for gas production contained in this volume. The most important sources for radilytic gas production are already present fluids and the organic material. Moreover, gases such as hydrogen and methane will oxidize to produce wtaer and carbon dioxide in so far as oxygen is available.

REFERENCES

N. AKRAM, J.C. BLANCHARD, M.T. GAUDEZ, P. TOULHOAT, J. MÔNIG, J.M. PALUT , 1991 : radiolysis-induced gas generation and release from radioactive waste repositories". OECD/NEA workshop, Aix en Provence, France pp. 130-141.

N. AKRAM, J.C. BLANCHARD, M.T. GAUDEZ, P. TOULHOAT, 1992 : "*Compared study of radiolysis-induced gas liberation in rocksalts from various origins*". Boston RS symposium,Vol 294 pp 447-452.

N. AKRAM, 1993 : "*Phénoménologie de la radiolyse de sels: Aplication au stockage de déchets nucléaires de haute activité*". Ph.D. Thesis, Université de Paris VI. 22 June 1993, 291 pp.

D. GAUDIN and M.T. GAUDEZ, 1993 : "Identification et dosage de composés organiques formés lors de l'irradiation de matériaux salins" CEA report DCC/DSD/SCS 93.15

M.T. GAUDEZ, H. PITSCH, J. FLORESTAN, J.C. BOULOU, 1993 : "Multicomponent analysis of small volumes of gas mixtures : an original method for processing FITR spectra. 28 th symposium of spectroscopy, YORK (GB) 29 June-4 July 1993.